LBNL-1006472

TOGA: A TOUGH code for modeling three-phase, multi-component, and non-isothermal processes involved in CO_2-based Enhanced Oil Recovery

Lehua Pan

Curtis M. Oldenburg

Energy Geosciences Division
Lawrence Berkeley National Laboratory
University of California
Berkeley, CA 94720

October 10, 2016

This work was funded by the Assistant Secretary for Fossil Energy, Office of Coal and Power Systems through the National Energy Technology Laboratory, by Royalty Funds administered by the Energy Geosciences Division of LBNL, and by Lawrence Berkeley National Laboratory under Department of Energy Contract No. DE-AC02-05CH11231.

DISCLAIMER

Abstract

TOGA is a numerical reservoir simulator for modeling non-isothermal flow and transport of water, CO_2, multicomponent oil, and related gas components for applications including CO_2-enhanced oil recovery (CO_2-EOR) and geologic carbon sequestration in depleted oil and gas reservoirs. TOGA uses an approach based on the Peng-Robinson equation of state (PR-EOS) to calculate the thermophysical properties of the gas and oil phases including the gas/oil components dissolved in the aqueous phase, and uses a mixing model to estimate the thermophysical properties of the aqueous phase. The phase behavior (e.g., occurrence and disappearance of the three phases, gas + oil + aqueous) and the partitioning of non-aqueous components (e.g., CO_2, CH_4, and n-oil components) between coexisting phases are modeled using *K*-values derived from assumptions of equal-fugacity that have been demonstrated to be very accurate as shown by comparison to measured data. Models for saturated (water) vapor pressure and water solubility (in the oil phase) are used to calculate the partitioning of the water (H_2O) component between the gas and oil phases. All components (e.g., CO_2, H_2O, and *n* hydrocarbon components) are allowed to be present in all phases (aqueous, gaseous, and oil). TOGA uses a multiphase version of Darcy's Law to model flow and transport through porous media of mixtures with up to three phases over a range of pressures and temperatures appropriate to hydrocarbon recovery and geologic carbon sequestration systems. Transport of the gaseous and dissolved components is by advection and Fickian molecular diffusion. New methods for phase partitioning and thermophysical property modeling in TOGA have been validated against experimental data published in the literature for describing phase partitioning and phase behavior. Flow and transport has been verified by testing against related TOUGH2 EOS modules and CMG. The code has also been validated against a CO_2-EOR experimental core flood

involving flow of three phases and 12 components. Results of simulations of a hypothetical 3D CO_2-EOR problem involving three phases and multiple components are presented to demonstrate the field-scale capabilities of the new code. This user guide provides instructions for use and sample problems for verification and demonstration.

This page left intentionally blank.

Contents

List of Figures

List of Tables

This page left intentionally blank.

1. Introduction

Partially depleted oil and gas reservoirs are excellent potential storage sites for carbon dioxide (CO_2) as suggested by their demonstrated long-term capability to store hydrocarbons. After primary and secondary recovery operations, an oil reservoir could still contain 60 - 85% of the original oil in place, which often invites enhanced oil recovery (EOR), which includes EOR by means of CO_2 injection (CO_2-EOR), a process that has been carried out profitably for over 40 years in the U.S. The enhancement of oil recovery and incidental trapping of CO_2 in CO_2-EOR make this process a promising large-scale utilization and sequestration approach provided the CO_2 is sourced from industrial operations, e.g., captured from fossil-fuel power plants (U.S. DOE, 2010). Critical to optimal CO_2-EOR with associated geologic carbon sequestration is the ability to simulate reservoir processes for design and operation of the CO_2-EOR reservoir where optimal oil recovery and long-term storage of CO_2 are objectives.

Numerical simulation of CO_2-EOR is much more challenging than simulating CO_2 storage in saline aquifers, mainly because an additional fluid phase (the non-aqueous oil-rich phase) and multiple additional components have to be considered. Although significant advancements in numerical simulation of CO_2-EOR processes have been achieved in the oil and gas industry in past decades and the development of related numerical simulators has grown into a specialized sub-industry, commercial codes are proprietary and their emphases are more on forecasting oil production and economic assessments of production without consideration for CO_2 trapping and CO_2 interactions with the water/brine phase. Here we present a new numerical simulator for the scientific investigation of CO_2 utilization and storage in partially depleted oil and gas reservoirs.

We present in Figure 1.1 a sketch of the processes that may attend CO_2-EOR in the reservoir, depending on pressure and temperature. As shown, the processes include multiphase (aqueous, CO_2, oil) and multicomponent (e.g., H_2O, NaCl, CO_2, oil, natural gas, and other co-constituents (e.g., H_2S)) and non-isothermal flow and transport. The key physical process that makes CO_2-EOR highly effective for oil recovery is the high solubility of CO_2 in oil at certain pressures and temperatures. This solubility is often referred to as miscibility, although CO_2 and oil are not formally miscible because they do not combine to form a single phase in all proportions (e.g., as water and ethyl alcohol do). The minimum pressure in the reservoir at a certain temperature is referred to as the minimum miscibility pressure (MMP). The most effective alteration in oil properties for oil recovery occurs when CO_2 dissolves into oil at or above the MMP, a process by which two phases (CO_2 and oil) combine to become a single phase that is more mobile than the original oil phase. When pressure drops below the MMP at a given temperature, CO_2 exsolves from the oil and two phase conditions return. In addition to solubility of CO_2 in oil, the H_2O is also soluble in the oil and CO_2 phases to a certain extent, as are hydrocarbon gases. In short, there are many solubility and phase (dis-) appearance processes that must be modeled to simulate CO_2-EOR and related potential CO_2 trapping and fluid migration (leakage) processes in the overburden. In fact, putting aside the multiphase flow aspects, the key feature of CO_2-EOR that must be captured in any simulator is mutual solubility of the various components (e.g., H_2O, n-oil components, n-oil vapors, non-condensible gases such as CH_4 and H_2S, and solvent fluids such as CO_2, and salt) in the various phases (aqueous, oil, and gas).

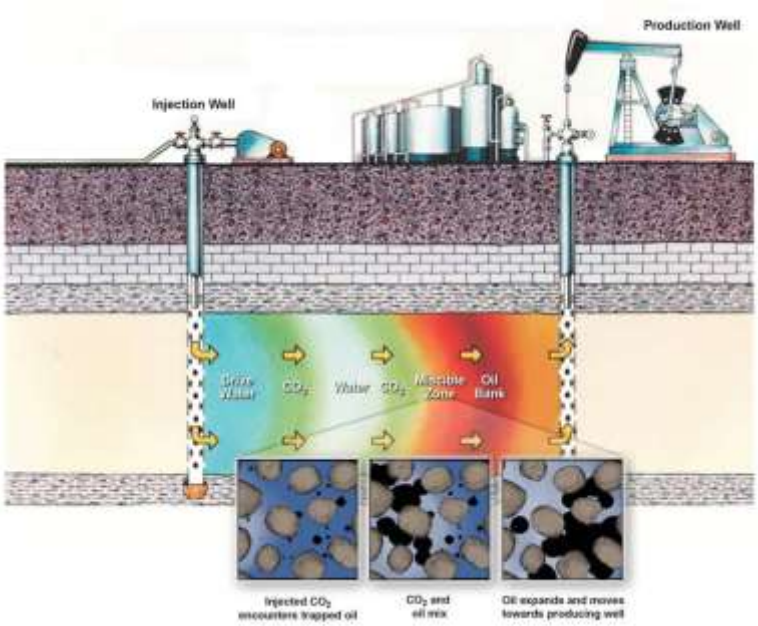

Figure 1.1. *Sketch of CO_2 injection into an oil reservoir for miscible CO_2-EOR. Some of the CO_2 dissolves into oil that remains after primary and secondary recovery. The CO_2 dissolved into oil causes oil to swell and become more mobile, while the rest of the CO_2 stays in the reservoir as sequestered CO_2 (from U.S. DOE, 2010).*

In order to carefully evaluate the potential of CO_2-EOR for both EOR and geologic carbon sequestration and to design injection and recovery strategies, we have developed a new reservoir simulator based on TOUGH2 that models full miscibility of CO_2 in oil and oil in CO_2 along with other significant processes relevant to CO_2-EOR and long-term CO_2 trapping in depleted hydrocarbon reservoirs. The code, TOGA (TOUGH Oil, Gas, Aqueous), is a new member of the TOUGH family of codes and is being made available to the research community by license just as other TOUGH developments are licensed at http://esd.lbl.gov/research/projects/tough/ This user guide describes the methods implemented in TOGA, shows results of testing to verify these methods, and provides sufficient information to run the code.

2. State of the Art of CO_2-EOR Simulation

The state of the art of CO_2-EOR simulators was recently reviewed in the thesis of Karacaer (Karacaer, 2013). To summarize Karacaer's review, there are several commercial reservoir simulators used by industry to model CO_2-EOR such as Eclipse-300® (Schlumberger), VIP-Comp® (Halliburton), GEM® (CMG), Sensor® (Coats Engineering) and MORE® (Roxar). Two end-member categories of CO_2-EOR simulators exist: (1) compositional, in which solubility of each component in each phase and the coupling of the dependence of solubility on composition is modeled; and (2) black oil, in which the oil phase does not volatilize and is not miscible with CO_2. Some simulators, e.g., Eclipse and CMG use an extended black oil formulation which considers three phases and four components (water, oil, hydrocarbon gas, and a solvent such as CO_2) and allows for dissolution of CO_2 into the oil to model miscibility. Commercial numerical reservoir simulators are proprietary codes that cost tens to hundreds of thousands of dollars to license or purchase. As commercial and proprietary codes, the source code, algorithms, and even the details of the models implemented are often opaque and not available for examination, scrutiny, or extension. The high cost and opacity of commercial software such as these codes make these existing CO_2-EOR capabilities effectively unavailable to the research community. The needs of the research community include the ability to modify the codes for specialized uses, test individual process modeling components, customize input and output, and most importantly, add in new process-modeling capabilities as they are developed, e.g., by the national labs.

There are two main government-funded research codes accessible to the research community to model processes and mechanisms relating to CO_2-EOR: (1) COZVIEW/COZSIM; and (2)

STOMP-EOR. Developed by NITEC LLC with funding from the National Energy Technology Laboratory (NETL), COZVIEW/COZSIM was developed for small to mid-size companies to enable relatively sophisticated feasibility assessments and net present value (NPV) estimates for CO_2-EOR in oil reservoirs. The methods are based on a technically rigorous three-dimensional, three-phase, four-component extended black oil simulator. As such, COZVIEW/COZSIM assumes the oil phase does not change composition and does not dissolve into the CO_2. The free version of COZVIEW/COZSIM requires that users follow a very difficult installation process. The other code available to researchers is STOMP-EOR (White and Oostrom, 2000; White et al., 2012). STOMP-EOR provides compositional, three-phase, and non-isothermal, geochemical, and geomechanical simulation capabilities. One limitation of STOMP-EOR is that aqueous phase is assumed to not dissolve in oil, an assumption not made in TOGA.

For applications ranging from optimal oil recovery under CO_2 injection, and optimal trapping of CO_2 in depleted oil reservoirs where water is abundant, we decided that water-oil miscibility was important and needed to be modeled along with full CO_2-oil mutual miscibility. TOGA was developed with focus on accurately modeling the solubility of the various components in all three potential phase, aqueous, gas, and oil.

3. Mathematical Formulation

3.1 Mass and energy conservation and flow

The general conservation equations solved in TOUGH2 for simulating multicomponent and multiphase flow and transport in porous media are well-known and presented in Pruess et al. (1999; 2012) along with a complete description of the theory and use of TOUGH2. Presented here for completeness, the general mass and energy conservation equation solved in TOUGH is

$$\frac{d}{dt}\int_{V_n} M^{\kappa} dV = \int_{\Gamma_n} \mathbf{F}^{\kappa} \cdot \mathbf{n} d\Gamma + \int_{V_n} q_v{}^{\kappa} dV \quad (3\text{-}1)$$

where the accumulation term is

$$M^{\kappa} = \phi \sum_{\beta=1}^{NPH} S_{\beta} \rho_{\beta} X_{\beta}^{\kappa} \quad (3\text{-}2)$$

and the component flux is

$$\mathbf{F}^{\kappa} = \sum_{\beta} X_{\beta}^{\kappa} \rho_{\beta} \mathbf{u}_{\beta} \qquad (3\text{-}3)$$

The term $\mathbf{u}_{\beta}$ in Eq. 3-3 is the Darcy velocity of phase β which is calculated using a multiphase version of Darcy's law

$$\mathbf{u}_{\beta} = -k \frac{k_{r\beta}}{\mu_{\beta}} \left(\nabla P_{\beta} - \rho_{\beta} \mathbf{g} \right) \qquad (3\text{-}4)$$

When applying Eq. 3-1 to energy conservation, the energy flux term and the energy accumulation terms are described by

$$\mathbf{F}^{\kappa} = -\lambda \nabla T + \sum_{\beta=1}^{NPH} h_{\beta} \rho_{\beta} \mathbf{u}_{\beta} \qquad (3\text{-}5)$$

$$M^{\kappa} = (1-\phi)\rho_{\beta} C_R T + \phi \sum_{\beta=1}^{NPH} \rho_{\beta} S_{\beta} U_{\beta} \quad (3\text{-}6)$$

Symbols are defined in the *Nomenclature* table at the end of this user guide.

3.2 Components

Table 3.1 provides a list of the components available in the internal data base of TOGA. While H_2O is the default component in any simulation, any combination of the other components is allowed. Hereafter, we will use the term "HC components" as a collective name for all of the components excluding water (H_2O) in a given system. This includes CO_2 and non-condensibles like H_2S, along with all of the formal hydrocarbon components (e.g., CH_4 (C1), etc.).

The user can also use hydrocarbon components other than those in the default data base by defining them in the input file as pseudo-components, provided that the parameters required in EOS are also included.

*Table **3.1.** Twenty-one components available in the internal data base of TOGA.*

Components	Symbol*	Components	Symbol*	Components	Symbol*
METHANE	CH4	WATER	H2O	n-HEPTANE	C7H16
ETHANE	C2H6	METHANOL	CH4O	n-OCTANE	C8H18
PROPANE	C3H8	n-BUTANE	C4H10	n-NONANE	C9H20
HYDROGEN SULFIDE	H2S	n-PENTANE	C5H12	n-DECANE	C10H22
CARBON DIOXIDE	CO2	n-HEXANE	C6H14	BENZENE	C6H6
NITROGEN	N2	i-BUTANE	iC4H10	SULPHUR DIOXIDE	SO2
OXYGEN	O2	i-PENTANE	iC5H12	NITROGEN OXIDES	NO2

* used to identify the component in the input file.

3.3 Thermophysical properties of non-aqueous phases (gas or oil)

TOGA uses thermophysical property models based on GasEOS (Reagan, 2006) as modified by Battistelli and Marcolini (2009). The Peng-Robinson (PR) cubic EOS (Peng and Robinson, 1976) given by

$$Z^3-(1-B)Z^2+\left(A-2B-3B^2\right)Z-\left(AB-B^2-B^3\right)=0 \quad (3\text{-}7)$$

is used to calculate the compressibility, Z, of non-aqueous (gas or oil) phases including the mixture of HC components dissolved in the aqueous phase. The coefficients A and B are functions of pressure and temperature for pure compounds with known parameters such as critical pressure (P_c), critical temperature (T_c), and the Pitzer acentric factor (ω). For fluid mixtures, they are also dependent on the composition. The binary interaction coefficients customarily used for the PR EOS have been taken from various bibliographic sources. Other parameters such as molecular weight, critical properties, acentric factor, and coefficients of specific heat of ideal gas are taken from the Property Data Base published by Poling et al.

(2000). The components included in the data base are H_2O, CO_2, N_2, H_2S, C1 through C10, including iC4 and iC5 (see Table 3.1). In addition, users have the option of using their own customized parameters including P_c, T_c, ω, molecular weight, and binary interaction coefficients as part of the input file.

In the case that Eq. 3-7 has multiple roots, the stability criterion suggested by Nghiem and Li (1989) is used to select the stable Z according to the difference of dimensionless free energy of the smallest root (Z_b) and the largest root (Z_a):

$$dG = Z_a - Z_b + \ln\left(\frac{Z_b - B}{Z_a - B}\right) + \frac{A}{B(\delta_2 - \delta_1)} \ln\left[\left(\frac{Z_b + \delta_2 B}{Z_a + \delta_2 B}\right)\left(\frac{Z_a + \delta_1 B}{Z_b + \delta_1 B}\right)\right] \quad (3\text{-}8)$$

where $\delta_1 = 1 + \sqrt{2}$ and $\delta_2 = 1 - \sqrt{2}$. Z_b is selected if $dG > 0$, otherwise Z_a is selected. However, if the phase is knownapriori, the smallest root will be selected for the oil phase and the largest root will be selected for the gas phase.

The gas or oil phase density is then calculated as:

$$\rho = \frac{P}{ZRT} \quad (3\text{-}9)$$

The volume-shift technique proposed by Péneloux et al. (1982) is used to improve the predicted phase density without affecting the phase equilibrium calculations.

The specific enthalpy, h, of the mixture at given P and T is calculated as a summation of the enthalpy changes of two processes from the triple point of water to the current point (T, P). The first process accounts for enthalpy changes assuming ideality by the equation

$$h(T, P) = h_{ideal}(T, P_{ref}) - \Delta h(T, P) \qquad (3\text{-}10)$$

where h_{ideal} is the specific enthalpy of the mixture at the low pressure (P_{ref} = 0.001 MPa) and current T, and is calculated as an ideal mixture of individual components by

$$h_{ideal}(T, P_{ref}) = \sum_i y_i h_i(T, P_{ref}) \qquad (3\text{-}11a)$$

where y_i is the mole fraction of the ith component and h_i is the specific enthalpy of the ith pure component. The specific enthalpy of pure component is calculated using the regression Eq. 3-11b established based on the temperature-dependent h values at P_{ref} obtained from NIST webbook (http://webbook.nist.gov/chemistry/fluid/). Figure 3.1 shows the comparison between the calculated specific enthalpy using

$$h_i = a_0 + a_1 T + a_2 T^2 + \frac{a_3}{T} \qquad \text{(3-11b)}$$

and the NIST data at various temperatures where a_0, a_1, a_2, and a_3 are the fitting parameters obtained by regression.

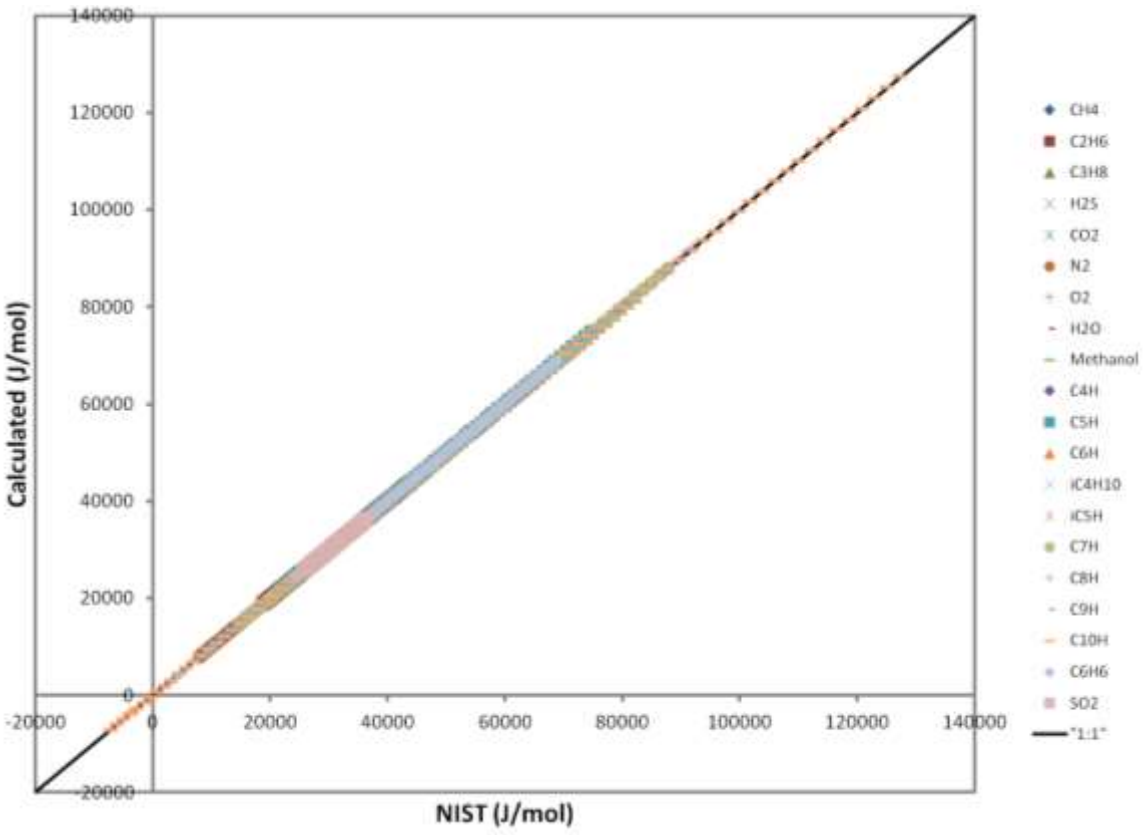

Figure 3.1. *Calculated specific enthalpy of individual components using Eq. 3-11b as compared to the data obtained from NIST webbook.*

The second part of the enthalpy calculation is the enthalpy departure, Δh, which accounts for the real mixing effect. The enthalpy departure is computed with a departure function derived from the model EOS, including derivatives of the EOS parameters as a function of temperature.

The viscosity of non-aqueous (gas or oil) phase is calculated as a function of given pressure, temperature, compressibility, and composition according to friction theory developed by Quiñones-Cisneros, et al. (2000). The same seven calibrated parameters used in TMGAS (Battistelli and Marcolini, 2009) are used here. In case that there are hypothetical HC

components, the viscosity of the mixture will be adjusted by the viscosity of the hypothetical HC components as:

$$\mu = x_h \mu_h + (1 - x_h)\mu_Q \qquad (3\text{-}12)$$

Where x_h is the total mole fraction of the hypothetical components in the phase whereas μ_Q is the viscosity of the mixture calculated using the Quiñones-Cisneros approach above. The viscosities of the hypothetical components, μ_h, are calculated as the reciprocal of the fluidity, f_h, following the method proposed by Davidson (1993):

$$\mu_h = \frac{1}{f_h} \qquad (3\text{-}13)$$

where the fluidity of the hypothetical components are defined as a combination of the viscosities of the individual hypothetical components:

$$f_h = \sum_{i=1}^{N_h} \sum_{j=1}^{N_h} \frac{\theta_i \theta_j E_{i,j}^A}{\sqrt{\mu_i \mu_j}} \qquad (3\text{-}14)$$

where N_h is the number of hypothetical components and μ_i is the viscosity of i^{th} hypothetical component, which is calculated using Arrhenius-type equation (the subscript 'i' is dropped for simplicity):

$$\mu = \mu^0 \left[1 + \alpha\left(P - P^0\right)\right] \exp\left(\frac{E_P}{RT}\right) \qquad (3\text{-}15)$$

In Eq. 3015, the reference viscosity, μ^0 , the reference pressure, P^0 , the pressure coefficient, α, and the "activation energy", E_p of the given hypothetical component are parameters provided by the user through the definition of the component in the input file.

The momentum fraction of the i^{th} component, θ_i, in equation (3-14) is defined as a function of mole fraction, x_i, and molecular weight, M_i, of the i^{th} component:

$$\theta_i = \frac{x_i \sqrt{M_i}}{\sum_{i=1}^{N_h} x_i M_i} \qquad (3\text{-}16)$$

The mean efficiency of the interaction between i^{th} and j^{th} components, $E_{i,j}$, in equation (3-14) is defined as:

$$E_{i,j} = \frac{2\sqrt{M_i M_j}}{M_i + M_j} \qquad (3\text{-}17)$$

The only empirical parameter, A, in equation (3-14) is fixed at 0.375 as suggested by Davidson (1993) and is applied to all hypothetical components.

3.4 Thermophysical properties of aqueous phase

For the aqueous phase, the density is calculated assuming additive volumes of pure water and dissolved CO_2 only:

$$\rho_{aq} = \frac{1}{x_{CO2} / \rho_{CO2} + (1 - x_{CO2}) / \rho_W} \qquad (3\text{-}18)$$

where x_{CO2} is the mole fraction of CO_2 component in aqueous phase, ρ_w is the density of pure water, and ρ_{CO2}, is the density of CO_2 which is calculated as a function of temperature from the correlation for molar volume of dissolved CO_2 at infinite dilution developed by García (2001).

$$V_\phi = a + bT + cT^2 + dT^3 \qquad (3\text{-}19)$$

In Eq. (3-19), molar volume of CO_2 is in units of cm^3 per gram-mole, temperature T is in ˚C, and a through d are fitting parameters given in Table 3.2.

Table 3.2. Parameters for molar volume of dissolved CO_2 (Eq. 3-19)

a	37.51
b	-9.585e-2
c	8.740e-4
d	-5.044e-7

The partial density of dissolved CO_2 in units of kg/m^3 is then

$$\rho_{CO2} = \frac{M_{CO2}}{V_\phi} \times 10^3 \qquad (3\text{-}20)$$

where M_{CO2} is the molecular weight of CO_2.

.

The effects of other dissolved components on the density of the aqueous phase are ignored.

The specific enthalpy of aqueous phase is calculated as:

$$h_{aq} = u_{H2O} + \frac{P}{\rho_{aq}} \qquad (3\text{-}21)$$

where u_{H2O} is the internal energy of pure water calculated using steam table formulation. The effects of the dissolved non-aqueous components on the specific enthalpy of the aqueous phase are also ignored except insofar as they enter through the density calculated in equation (3-18).

The viscosity of the aqueous phase is simply calculated as pure water (ASME, 1977, Gallagher & Kell, 1984).

3.5 Interfacial tension between gas and oil phases

Interfacial tension between gas and oil phase σ_{go} is calculated using the parachor model (Weinaug and Katz, 1943):

$$\sigma_{go} = \left(\rho_o \sum x_o^i P_i - \rho_g \sum x_g^i P_i\right)^4 \qquad (3\text{-}22)$$

Where ρ_o and ρ_g are densities of the oil phase and the gas phase, respectively. The parachor of the i^{th} component P_i is listed in Table 3.3 for common HC components which are included in the internal data base.

Table 3.3. Parachor of various components

Component	Parachor
N_2	41.0
CO_2	78.0
H_2S	80.1
C1	77.0
C2	108.0
C3	150.3
iC4	181.5
nC4	203.4
iC5	225.0
nC5	231.5
C6	271.0
C7	312.5
C8	351.5
C9	393.0
C10	446.2

For those components not listed in Table 3.3, its parachor is calculated as a function of its molecular weight (Firoozabadi et al., 1988):

$$P_i = -11.4 + 3.23M_i - 0.0022M_i^2 \qquad (3\text{-}23)$$

Where M_i is the molecular weight (in gram moles) of component i.

4. Approach to Model Three-Phase System

4.1 Primary variables and phase conditions

As shown in Table 4.1, TOGA uses three different sets of primary variables to describe three groups of the possible phase conditions, namely, non-aqueous phase only (CID = 1), aqueous phase only (CID = 2), and two phases (CID = 3). The non-aqueous phase could be either gas-only (G), oil-only (O), or gas + oil (G + O) two phases, depending on the given *P*, *T*, and composition of HC components. Similarly, the two-phase condition (W + N) could actually be either aqueous and gas phase (W + G), aqueous and oil (W + O), or three phase (W + G + O). As a result, totally seven phase combinations are simulated.

Table 4.1. *Primary variables used by TOGA.*

<table>
<tr><td colspan="4">Phase conditions</td><td colspan="4">Primary variables</td></tr>
<tr><td>Phase category</td><td>CID</td><td>PID</td><td>Actual Phase</td><td>1</td><td>2</td><td>3 to NHC+1</td><td>NHC+2</td></tr>
<tr><td rowspan="3">Non-aq only</td><td rowspan="3">1</td><td>1</td><td>Gas only (G)</td><td rowspan="3">P</td><td>X_g^W</td><td rowspan="4">$Z_i (i \neq j)$</td><td rowspan="4">T</td></tr>
<tr><td>3</td><td>Oil only (O)</td><td rowspan="2">X_g^{HC}</td></tr>
<tr><td>5</td><td>Gas and oil (G + O)</td></tr>
<tr><td>Aqueous only</td><td>2</td><td>2</td><td>Water only (W)</td></tr>
<tr><td rowspan="3">Two or more phases</td><td rowspan="3">3</td><td>4</td><td>Water and gas (W + G)</td><td rowspan="3">P (isothermal) or P_{HC} (non-isothermal)</td><td rowspan="3">S_w</td></tr>
<tr><td>6</td><td>Water and oil (W + O)</td></tr>
<tr><td>7</td><td>Three phase (W + G + O)</td></tr>
</table>

The number of primary variables is flexible and is dependent of the number of HC components, NHC, involved in the given system. The mole fraction of water, X_g^W, and the total mole fraction

of all HC components, X_g^{HC} , comprise the (hypothetical) gas phase. The aqueous phase saturation is denoted S_w.. The above three variables are the possible options for the second primary variable which needs to be switched if phase conditions change.

The primary variable, z_i, is defined as the mole fraction of the ith HC component in the HC mixture (excluding water) which could be in either gas, oil, or gas + oil phases:

$$z_i = \frac{mole_i^{HC}}{\sum_{k=1}^{NHC} mole_k^{HC}} \qquad (4\text{-}1)$$

As shown in Table 4.1, totally NHC-1 primary variables are needed to describe the composition of the HC mixture. The component that is not included in the primary variables is called the "*J*-component" whose mole fraction, z_j, can be obtained from the other primary variables z_i (i = 1, NHC; $i \neq j$) as:

$$z_j = 1 - \sum_{i=1, i \neq j}^{NHC} z_i \qquad (4\text{-}2)$$

TOGA will check if z_j is large than a predefined value for every grid cell before the next time step. If not, TOGA will pick the component with the largest mole fraction as the new "*J*-component" and make the necessary switch of the primary variables. In this way, we can avoid the trouble of "negative mole fractions" in EOS calculations.

The first primary variable in TOGA is usually the total pressure with the exception of the case in which the water phase is in equilibrium with one or more non-aqueous phases (Category 3) in a

non-isothermal simulation, in which case the first primary variable is the partial pressure of HC components in the (hypothetical) gas phase, P_{HC},.. This approach has been shown to be better in handling the simulation of systems with steam injection where the gas phase is composed mostly of water vapor, in which case *P* and *T* are interdependent, although the current implementation of phase partitioning method still limits the applications involving three phase system at the boiling point of water.

4.2 Equilibrium mole fractions and phase partitioning

4.2.1 Water in gas or oil phase

Approaches to modeling the phase partitioning of water between gas and oil phases are needed to simulate CO_2 and oil flow and transport for EOR and geologic carbon sequestration. In TOGA, we assume the following:

1. The equilibrium mole fraction of water in the gas phase can be calculated as the ratio of saturated vapor pressure at given *T* and the total pressure:

$$x^{W}_{g,\,eq} = \frac{P_{sat}(T)}{P} \qquad (4\text{-}3)$$

2. The equilibrium mole fraction of water in the oil phase is controlled by the temperature-dependent solubility adjusted by the pressure:

$$x^{W}_{o,\,eq} = WsoluO(T)\frac{P_0}{P} \qquad (4\text{-}4)$$

Where P_0 (= 1 atm) is the reference pressure.

3. The effects of water in either gas phase or oil phase on the partitioning coefficient (*K*-value) of HC components between non-aqueous phases are negligible.

With above approximations, we can determine the water mole fraction in each of non-aqueous phases as follows.

If the aqueous phase exists, the total mole fractions of water in gas and oil phases are simply the equilibrium values as defined in (Eqs. 4-3 and 4-4) in each phase:

$$\begin{aligned} x_g^W &= x_{g,eq}^W \\ x_o^W &= x_{o,eq}^W \end{aligned} \qquad (4\text{-}5)$$

If aqueous phase does not exist, the mole fraction of water in the gas phase, x_g^W, is known as one of the primary variables. Therefore, the mole fraction of water in the oil phase, x_o^W, can then be calculated as:

$$x_o^W = x_g^W \frac{x_{o,eq}^W}{x_{g,eq}^W} \qquad (4\text{-}6)$$

Note that the primary variable, x_g^W would be referred to the hypothetical gas phase (i.e., summation of mole fractions ≤ 1) which is in equilibrium with the given oil phase in the case that the non-aqueous phase is actually a single oil phase.

4.2.2 Calculation of the K-value (partition coefficient of HC components between Gas and oil phases)

The *K*-values are equilibrium ratios of the HC component mole fractions in the gas phase divided by mole fractions in the oil phase

$$K_i = \frac{y_i}{x_i} \qquad (4\text{-}7)$$

where y_i and x_i are mole fractions of the i^{th} HC component in the gas phase and in the oil phase. There are two approaches to calculate the *K*-values in TOGA. The first one is based on an empirical model of *K*-value. The second one is a more thermophysically consistent approach (often called flash calculation) which needs iterative calculations of the *K*-values based on updated applications of the EOS equations until the fugacity in both phases becomes equal. Users can select to use the simple non-iterative "*K*-value" approach by setting IE(8) = 1 in the SELEC block of the TOUGH2 input file or use the iterative "flash" approach by setting IE(8) > 1. The value of IE(8) in the input file is used as the maximum number of iterations of the "flash" calculation.

The following are detailed descriptions of these methods.

First, the *K*-value method is based on the new empirical *K*-value equation proposed by Ghafoori et al. (2012) for reservoir fluids which shows good agreement to 122 sets of experimental bubble pressure data. The modified Whitson equation implemented in TOGA is:

$$K_i = \left(\frac{1}{P_{ri}}\right)^{\beta} \exp\left[\varepsilon\,\beta(1+\omega)\left(1-T_{ri}^{-1}\right)\right] \qquad (4\text{-}8)$$

where P_{ri} (= P/P_{ci}) and T_{ri} (= T/T_{ci}) are reduced pressure and reduced temperature of component i, and β is defined as

$$\beta = 1 - \left(\frac{P}{P_k}\right)^{\frac{T}{\sum z_i T_{ci}}} \qquad (4\text{-}9)$$

where P_k is the convergence pressure and T_{ci} is the critical temperature of component i. The constant ε in Eq. 4-8 was 5.37 in the original model (Ghafoori et al., 2012, Eq. 13). We use 5.6916 which was found to produce the smallest average errors at measured bubble pressures from the 122 sets of experimental data.

The second approach is mainly based on the method proposed by Michelsen (1982) which uses a type of procedure presented by Rachford and Rice (1952). This procedure involves iterative calculations of the K-values based on updated applications of the EOS equations until the fugacity in both phases becomes the same:

$$f_{g,i} = f_{o,i} \qquad i = 1, \cdots, NHC \qquad (4\text{-}10)$$

Eq. 4-10 can also be expressed using fugacity coefficient, ϕ_i, as:

$$\phi_{g,i} P y_i = \phi_{o,i} P x_i \qquad i = 1, \cdots, NHC \tag{4-11}$$

Combining Eq. 4-7 and 4-11, we can get:

$$K_i = \frac{\phi_{o,i}}{\phi_{g,i}} \tag{4-12}$$

The mole fractions, x_i and y_i, have following material balance relationships with the overall mole fraction z_i:

$$z_i = \left(1 - a_g\right) x_i + a_g y_{\mathrm{i}} \tag{4-13}$$

where a_g is the ratio of the total moles of HC components in the gas phase, n_g, over total moles of HC components, $n_g + n_o$, i.e.,

$$a_g = \frac{n_g}{n_g + n_o} \tag{4-14}$$

By inserting Eq. 4-7 into Eq. 4-13, we can determine x_i and y_i as a function of a_g, K_i, and z_i:

$$\begin{aligned} x_i &= \frac{z_i}{1 + a_g\left(K_i - 1\right)} \\ y_i &= \frac{K_i z_i}{1 + a_g\left(K_i - 1\right)} \end{aligned} \tag{4-15}$$

The ratio a_g can be solved from the summation of the mole fraction relation

$$\sum_{i=1}^{NHC}(y_i - x_i) = \sum_{i=1}^{NHC}\frac{z_i(K_i - 1)}{1 + a_g(K_i - 1)} = 0 \qquad (4\text{-}16)$$

We define a phase function $f(a_g)$ from Eq. 4-16 as

$$f(a_g) = \sum_{i=1}^{NHC}\frac{z_i(K_i - 1)}{1 + a_g(K_i - 1)} \qquad (4\text{-}17)$$

Because $z_i \geq 0$ and $K_i > 0$, $f(a_g)$ is a monotonically decreasing function of a_g. The value of a_g should be between 0 and 1. Therefore, for a given set of K_i and z_i, the case where $f(0) \leq 0$ indicates that the HC mixture forms a pure oil phase so that $x_i = z_i$. On the other hand, $f(1) \geq 0$ indicates that the HC mixture forms a pure gas phase so that $y_i = z_i$. For all other cases (except for $K_i = 1$ for all components), we solve $f(a_g) = 0$ to obtain a_g using hybrid bi-section and Newton iteration method (Press et al., 1992). The case of $K_i = 1$ (i.e., the trivial solution) usually indicates that the pressure reaches or passes the minimum miscibility pressure (MMP) and the system will be in single phase. If this is the case, TOGA will determine the phase (gas or oil) based on the total mole fraction of heavy (C4 and plus) components (e.g., oil phase if > 0.25).

With the relationships above, the flash calculation used in TOGA proceeds along the following steps:

Step 1: Calculate K_i using Ghafoori's equation Eq. 4-8 as initial guess;
Step 2: Obtain a_g by solving Eq. 4-16 with known K_i;
Step 3: Calculate y_i and x_i using Eq. 4-15 with the a_g obtained in Step 2;
Step 4: Calculate fugacity coefficients, $\phi_{g,i}$ and $\phi_{o,i}$ using EOS model with known y_i and x_i obtained in Step 3;
Step 5: Update K_i using Eq. 4-12;
Step 6: if $\sum(\ln(K_i)^2 \le 10^{-4}$, end iteration (trivial solution), otherwise go to Step 7;
Step 7: if $\sum\left(\frac{K_i}{K_{old,i}}-1\right)^2 \le 10^{-10}$, end iteration (convergent), otherwise go to Step 2.

If a_g obtained in Step 2 is less than or equal to zero, the oil phase will be tested to see if it is stable following the similar approach presented by Whitson and Brule (2000). If it is stable, the oil-only condition is identified and the flash calculation ends with $x_i = z_i$. Similar testing will be performed for the gas-only case for which a_g obtained in Step 2 is larger or equal to one. The testing procedure is similar to the steps described above but the "trial phase" may be a hypothetical phase. The following describes the steps to test if the oil phase is a stable single phase (the gas phase is the "trial phase"):

Step 1: Set $x_i = z_i$ and then calculate the oil phase fugacity coefficients, $\phi_{o,i}$;
Step 2: Calculate $Y_i = K_i z_i$ and obtain $S_v = \sum Y_i$;
Step 3: Get mole fraction in the trial phase, $y_i = \frac{Y_i}{S_v}$;
Step 4: Calculate the trial phase fugacity coefficients, $\varphi_{g,i}$;
Step 5: Update K_i using Eq. 4-12;
Step 6: if $\sum(\ln(K_i)^2 \le 10^{-4}$, end testing (trivial solution), otherwise go to Step 7;
Step 7: if $\sum\left(\frac{K_i}{K_{old,i}}-1\right)^2 \le 10^{-10}$, end testing (convergent), otherwise go to Step 2.

If the test converges to a trivial solution or the convergent $S_v < 1$, the single phase oil is stable. The testing steps for checking if the single gas phase is stable are similar except that the "trial" phase and the real phase are switched.

The resulting K_i will be used to calculate the mole fractions of HC components in each of non-aqueous phases as described in the following section.

4.2.3. Calculation of the mole fractions of HC components in the gas and oil phases with dissolved water

Although the effects of the water are ignored in determining the partition coefficients of HC components between gas and oil phase, we have to include the (possible) dissolved water in the non-aqueous phases in the determination of the actual mole fractions of HC components as well as the mole ratio A_g or volumetric gas saturation S_g. To do so, we start by rewriting the material balance relationship (Eq. 4-13) considering the existing water:

$$z_i^* = \left(1 - a_g^*\right) x_o^i + a_g^* x_g^i \qquad (4\text{-}18)$$

Where x_o^i, x_g^i, and z_i^* are mole fraction of the i^{th} HC component in oil, gas, and entire non-aqueous phase, respectively. The z_i^* can be obtained from the mole fractions z_i by including the total water mole fraction in the non-aqueous phase, z_0 (summation of water in oil phase and gas phase), where

$$z_i^* = \frac{z_i}{\sum_{i=1}^{NHC} z_i + z_0} = \frac{z_i}{1 + \left(1 - a_g^*\right) x_o^W + a_g^* x_g^W} \qquad (4\text{-}19)$$

The mole ratio in Eqs 4-18 and 4-19 now is defined as:

$$a_g^* = \frac{n_g + n_g^W}{n_g + n_g^W + n_o + n_o^W} \qquad (4\text{-}20)$$

Because we ignore the effects of water on the partition coefficients of HC components between gas and oil phases, we still have (with known K_i):

$$x_g^i = K_i x_o^i \qquad (4\text{-}21)$$

By inserting Eq. 4-20 into Eq. 4-18, we obtain:

$$x_o^i = \frac{z_i^*}{1+a_g^*\left(K_i-1\right)}$$
$$x_g^i = \frac{K_i z_i^*}{1+a_g^*\left(K_i-1\right)} \qquad (4\text{-}22)$$

As a result, we can have a relationship similar to Eq. 4-16:

$$\sum_{i=1}^{NHC}\left(x_g^i - x_o^i\right) = \sum_{i=1}^{NHC}\frac{z_i^*\left(K_i-1\right)}{1+a_g^*\left(K_i-1\right)} = x_o^W - x_g^W \qquad (4\text{-}22)$$

Finally, we can construct a phase function from Eq. 4-22 using the relationship in Eq. 4-19:

$$f\left(a_g^*\right) = \sum_{i=1}^{NHC}\frac{z_i\left(K_i-1\right)}{1+a_g^*\left(K_i-1\right)} + \left(x_g^W - x_o^W\right)\left[1+\left(1-a_g^*\right)x_o^W + a_g^* x_g^W\right] \qquad (4\text{-}23)$$

The same hybrid bi-section and Newton iteration method (Press et al., 1992) is used to obtain a_g^* by solving $f\left(a_g^*\right)=0$. The mole fractions of HC components can then be calculated using Eq. 4-22.

4.2.4. Calculation of the volumetric saturation of gas and oil phases

The volumetric saturations of the gas and oil phases can be calculated as:

$$S_g = \frac{a_g^* V_g}{a_g^* V_g + \left(1-a_g^*\right)V_o}\left(1-S_w\right)$$
$$S_o = \frac{\left(1-a_g^*\right)V_o}{a_g^* V_g + \left(1-a_g^*\right)V_o}\left(1-S_w\right) \qquad (4\text{-}24)$$

Where V_g and V_o are mole volume (m^3/mole) of gas and oil phases, respectively, which can be easily calculated from the density of the mixture. S_w is water saturation which is either zero (non-aqueous phase only) or the primary variable. Note that, in this framework, S_g and

S_o are always secondly variables whereas S_w may be the primary variable if aqueous and non-aqueous phases coexist.

4.2.5. Calculation of the mole fractions of HC components in the aqueous phase

The mole fractions of HC components in the aqueous phase are calculated based on assumed equilibrium between gas and aqueous phases. We use a two-step approach to calculate the actual mole fractions of the HC components in the aqueous phase. First (solubility stage), we calculate the mole fractions of HC components in the aqueous phase, x_i, corresponding to the given P, T, and the "scaled" mole fractions of HC components in gas phase, y_i. If the gas phase is real, y_i simply equals x_g^i. Otherwise (the gas phase is hypothetical), y_i is defined as follow:

$$y_i = \frac{x_g^i}{\sum_{i=1}^{NHC} x_g^i}\left(1 - x_g^W\right) \qquad (4\text{-}25)$$

We calculate x_i based on the relationship between the "true" equilibrium constant and the ratio of fugacity over activity of the i^{th} HC components:

$$K_i = \frac{\phi_{g,i} P y_i}{\gamma_i x_i} \qquad i = 1, \ldots, NHC \qquad (4\text{-}25)$$

The "true" equilibrium constants K_i are calculated as functions of given pressure and temperature using SUPCRT92 (Johnson et al., 1992) and the slop98 database from Shock (Geopig webpage). The activity coefficient, γ_i,in (4-25) is calculated by considering salting-out effects following the approaches suggested by Cramer (1982), Drummond (1981), and Soreide and Whitson (1992) for various components. Because the salt is not considered in the current version of the code, the activity coefficient is equal to one for all dissolved components.

Secondly, we obtain the actual mole fractions of HC components, x_a^i as:

$$x_a^i = x_g^i \frac{x_i}{y_i} \qquad (4\text{-}26)$$

4.3 Logic of primary variable and phase switching

As shown in Table 4.1, the 2nd primary variable will change according to the prevailing phase conditions. There are three phase categories. A phase occurring or disappearing can be determined based on the value of the 2nd primary variable as follows:

1) Non-aqueous only (N): (x_g^W is the 2nd primary variable)

   The condition for water phase to appear is $x_g^W P > \gamma P_{sat}$ ($\gamma > 1$ makes a finite window). If so, the 2nd primary variable will be switched to S_w set to a small value (e.g., 1×10^{-6}); the 1st primary variable will also be switched to P_{HC} if non-isothermal simulation is being carried out.

2) Aqueous only (W): (x_g^{HC} is the 2nd primary variable)

   First determine the phase composition of the hypothetical non-aqueous phase based on the given P, T, and z_i. If the hypothetical non-aqueous phase is oil only, the total mole fraction in the hypothetical phase, x_n, is calculated as that in the oil phase by

$$x_n = \frac{x_G^{HC}}{K_{GO}^{HC}} + x_{o,eq}^{w} \qquad (4\text{-}27)$$

Otherwise, if the hypothetical non-aqueous phase is gas or a mixture of gas-oil phases, the total mole fraction in the hypothetical phase is calculated as that in the gas phase:

$$x_n = x_G^{HC} + x_{G,eq}^{w} \qquad (4\text{-}28)$$

The condition for appearance of non-aqueous phase is $x_n > \gamma$ ($\gamma > 1$ makes a finite window). If so, the 2nd primary variable will be switched to S_w (e.g., 0.999999); the 1st primary variable will also be switched to P_{HC} if a non-isothermal simulation is being carried out.

3) Two phase: N+W (S_w is the 2nd primary variable)

The phase switch conditions are as follows:

$S_w \leq 0$: water phase disappears and the 2nd primary variable will be switched to x_g^W; the 1st primary variable will be switched to $P\ (=Psat + P_{HC})$ if non-isothermal simulation is being carried out.

$S_w \geq 1$: non-aqueous phase disappears and the 2nd primary variable will be switched to x_g^{HC}, the total mole fraction of the HC components in the hypothetical gas phase; the 1st primary variable will be switched to P if non-isothermal simulation is being carried out.

4.4 Three-phase relative permeability

The existence of three-phase conditions in reservoirs requires the ability to approximate three-phase relative permeability. Various three-phase relative permeability models are implemented in TOGA. Some are just simple extensions of two-phase (gas and water) relative permeability functions inherited from the TOUGH2 code (e.g., taking "gas" relative permeability as non-aqueous phase relative permeability and then splitting it by relative saturation of gas phase in the non-aqueous phase). The others are taken from literature and defined explicitly for three phase conditions. In the following we describe briefly two typical relative permeability models implemented in TOGA. The first is the STONE II model that assumes the oil relative permeability can be estimated from the relative permeabilities of water-oil and oil-gas systems which are provided in tabular input data. The second is the Coats model that calculates relative permeability of each phase using functions with parameters specified in the input file. The other two models that require tabular data input are STONE I (IRP = 14) and Baker (IRP = 16) models. All other models require parameter input.

4.4.1. STONE II model (IRP =15, tabular data input)

This model for the oil relative permeability was originally proposed by Stone (1973). The model implemented in TOGA is the normalized form suggested by Aziz and Settari (1979):

$$k_{ro}\left(S_w, S_g\right) = k_{rocw}\left[\left(\frac{k_{row}}{k_{rocw}} + k_{rw}\right)\left(\frac{k_{rog}}{k_{rocw}} + k_{rg}\right) - \left(k_{rw} + k_{rg}\right)\right] \qquad (4\text{-}29)$$

Where k_{rocw} is oil relative permeability at connate water saturation (S_{wc}), k_{row} is oil relative permeability at S_w when S_g=0, k_{rw} is water relative permeability as a function of S_w, k_{rog} is oil relative permeability at S_g when S_w=S_{wc}, k_{rg} is gas relative permeability as a function of S_g. All these two phase relative permeabilities are obtained by interpolation of the tabular data using a smooth monotonic interpolation method developed by Steffen (1990). If the oil relative permeability evaluated in Eq. 4-29 becomes less than zero, it is forced to be zero.
In TOGA, the water saturation could become smaller than the connate water saturation because the water could be carried away by the flowing gas/oil phase which causes local dry out of formation. In this case (i.e., $S_w < S_{wc}$), if the specified oil relative permeability, k_{rocw}, is less than 1, the two-phase relative permeabilities will be adjusted before using Eq. 4-29 to calculate the oil relative permeability as follows:

$$
\begin{aligned}
k_{rog}^{new} &= k_{rog}^{old} + \left(1 - k_{rocw}^{old}\right)\left(1 - \frac{S_w}{S_{wc}}\right) \\
k_{rg}^{new} &= k_{rg}^{old} + \left(1 - k_{rgc}^{old}\right)\left(1 - \frac{S_w}{S_{wc}}\right) \\
k_{row}^{new} &= k_{row}^{old} + \left(1 - k_{rocw}^{old}\right)\left(1 - \frac{S_w}{S_{wc}}\right) \\
k_{rocw}^{new} &= k_{rocw}^{old} + \left(1 - k_{rocw}^{old}\right)\left(1 - \frac{S_w}{S_{wc}}\right)
\end{aligned}
\qquad (4\text{-}30)
$$

Where superscript "old" indicates the values originally obtained from the interpolation of the tabular data whereas "new" indicates the adjusted value.

4.4.2. Coats model (IRP =13, parameters specified in input)

The Coats (1980) model which approximates gas phase relative permeability by the relation

$$k_{rg} = k_{rgcw}\left[\left(f(\sigma)\overline{S_g}^{n_g} + (1 - f(\sigma))\overline{S_g}\right)\right] \qquad (4\text{-}31)$$

While the oil phase relative permeability is given by

$$k_{ro} = k_{rocw}\left[\left(k_{row} + k_{rw}\right)\left(k_{rog} + k_{rg}\right) - k_{rw} - k_{rg}\right] \qquad (4\text{-}32)$$

and the relative permeability of the aqueous phase is given by

$$k_{rw} = k_{rwro}\left[\left(\frac{S_w - S_{wir}}{1 - S_{wir} - S_{orw}}\right)\right]^{n_w} \qquad (4\text{-}33)$$

The oil-water relative permeability is given by

$$k_{row} = \left(\frac{1 - S_w - S_{orw}}{1 - S_{wir} - S_{orw}} \right)^{n_{ow}} \tag{4-34}$$

and the oil-gas relative permeability is given by

$$k_{rog} = f(\sigma)\overline{S_o}^{n_{og}} + (1 - f(\sigma))\overline{S_o} \tag{4-35}$$

where

$$\overline{S_o} = \frac{1 - S_g - S_{wir} - S^*_{org}}{1 - S_{wir} - S^*_{org}} \tag{4-36}$$

$$\overline{S_g} = \frac{S_g - S^*_{gr}}{1 - S_{wir} - S^*_{gr}} \tag{4-37}$$

$$\begin{aligned} S^*_{gr} &= f(\sigma) S_{gr} \\ S^*_{org} &= f(\sigma) S_{org} \end{aligned} \tag{4-38}$$

where, $f(\sigma)$ is a function of surface tension, S_{wir} is the irreducible water saturation, S_{gr} is residual gas saturation, S_{org} is residual oil saturation to gas, S_{orw} is residual oil saturation to water, S_{rwro} is water relative permeability at residual oil saturation, k_{rocw} is oil relative permeability to

connate water saturation, and k_{rgcw} is gas relative permeability at connate water saturation. The terms n_w, n_{ow}, n_g, and n_{og} are the exponents of the relative permeability curves.

5. Verification of Component Phase Partitioning and Thermophysical Properties

5.1 Introduction

Due to the many processes modeled by TOGA, extensive testing and verification has been carried out to confirm that the code is performing as designed and in agreement with other codes and published data. In this section we summarize several of these tests.

5.2 Phase partitioning and properties of hydrocarbon mixture (C1-nC4-C10)

As emphasized throughout this report, the most important process controlling CO_2-EOR is the dissolution of gas components into oil and water and the associated changes in mixture properties (e.g., density and viscosity). A key parameter that controls the component distribution between phases is the partition coefficient (often called the *K*-value). In Figure 5.1 we show comparisons of *K*-values from TOGA against measured data from Sage and Lacey (1950) for the distribution of natural gas components into an oil proxy (C1 = methane = CH_4; nC4 = isobutene = C_4H_{10}; C10 = ndecane = $C_{10}H_{22}$). As shown, agreement is excellent. A subset of data are shown along with mole fractions in Table 5.1. We also show in Table 5.2 the excellent agreement in compressibility between TOGA and measured data of McCain (1990).

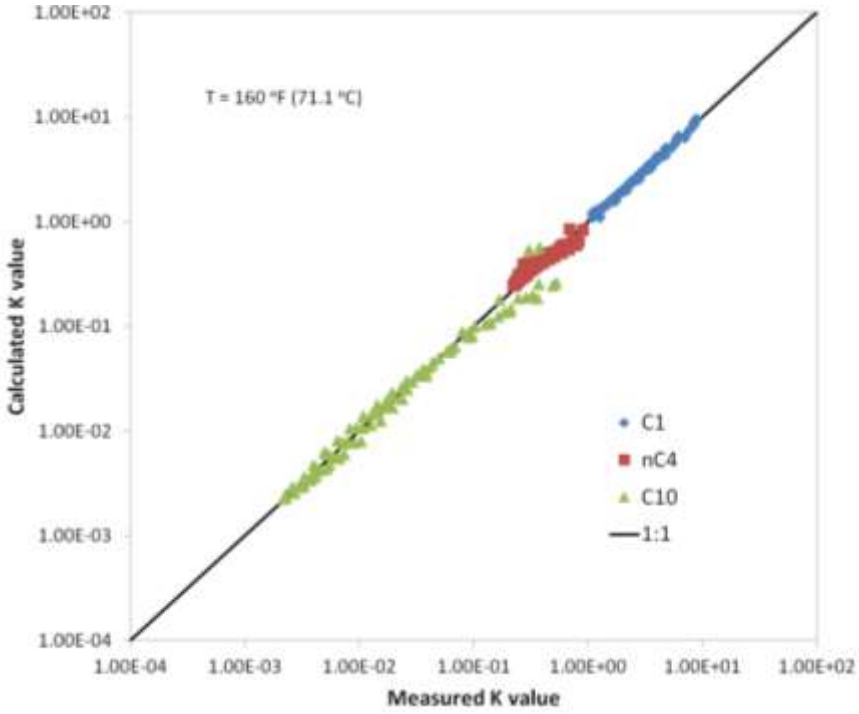

Figure 5.1. *Comparison of calculated K-values by TOGA against measured data (Sage and Lacey, 1950, Table 5-XIV) of hydrocarbon mixtures (C1-nC4-C10) under various pressure (400-5000 psi or 2.76-34.5 MPa) and compositions ($x_{nC4}/(x_{nC4}+x_{C10})$ = 0 to 1).*

Table 5.1. *Comparison of mole fractions and K-values of hydrocarbon mixture (C1-nC4-C10) at 1000 psi (6.89 MPa) and 160°F (71.1°C)*

Components	Overall mole fraction	Mole frac. (oil)		Mole frac. (gas)		*K*-value	
		Experimental data (Sage and Lacey 1950)	TOGA	Experimental data (Sage and Lacey 1950)	TOGA	Experimental data (Sage and Lacy, 1950)	TOGA
C1	0.5301	0.242	0.23979	0.963	0.9587	3.97934	3.99787
nC4	0.1055	0.152	0.15036	0.036	0.0393	0.23684	0.26113
C10	0.3644	0.606	0.60978	0.0021	0.0021	0.00347	0.00342

Table 5.2. *Comparison of phase compressibility factor of hydrocarbon mixture (C1-nC4-C10) at 1000 psi (6.89 MPa) and 160°F (71.1°C)*

phase	Oil	Gas
TOGA	0.3923	0.9030
McCain (1990)	0.3922	0.9051

5.3 Phase partitioning and properties of CO_2-hydrocarbon mixture (CO_2-nC4-C10)

The dissolution of CO_2 into oil and into water is of course the main process of interest in CO_2-EOR. Furthermore, oil and water dissolve into supercritical CO_2 and this process is also modeled in TOGA. We present in Table 5.3 the binary interaction coefficients used in the test problem, results of which are shown in Figures 5.2 and 5.3.

Table 5.3. *Binary interaction coefficients used in the test problem.*

	CO_2	nC4	C10
CO_2	0.0000E+00	8.6292E-02	9.7866E-02
nC4	8.6292E-02	0.0000E+00	3.3693E-08
C10	9.7866E-02	3.3693E-08	0.0000E+00

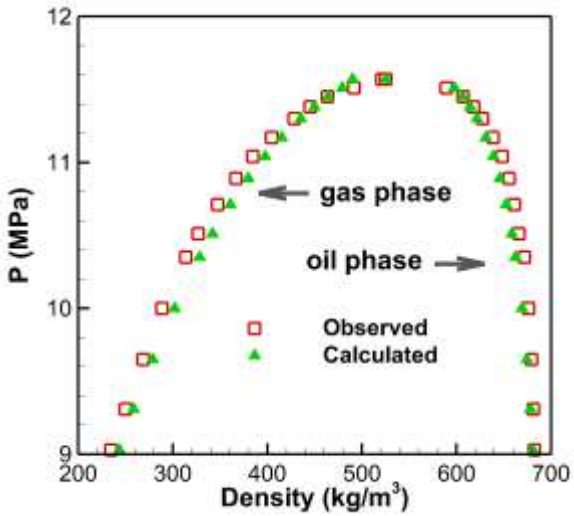

Figure 5.2. *Comparison of calculated phase density of CO_2-nC4-C10 mixture at 71.1°C and various pressures (9.03-11.6 MPa) against measured values from Nagarajan et al. (1990). Composition of the mixture: CO_2 (mole fraction = 0.902), nC4 (0.059), and C10 (0.039).*

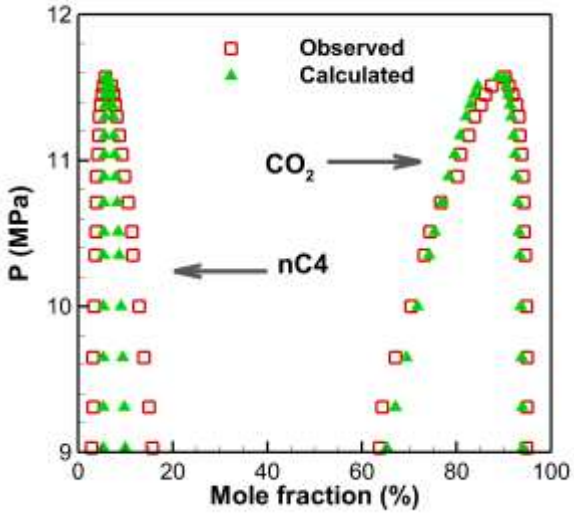

Figure 5.3. *Comparison of calculated mole fractions of CO_2 and nC4 in the equilibrium CO_2-hydrocarbon mixture at 71.1^oC and various pressures (9.03-11.6 MPa) against the measured values of Nagarajan et al. (1990). Composition of the overall mixture: CO_2 (mole fraction = 0.902), nC4 (0.059), and C10 (0.039).*

5.4 Thermophysical properties of gas (CO_2-rich phase)

Figure 5.4 shows comparisons of CO_2-H_2O mixture density calculated by TOGA and by other TOUGH2 codes (ECO2N and EOS7CMA) against measured data. ECO2N (default) uses an approach based on interpolation from empirical data, while TOGA and EOS7CMA are both based on equations of state, e.g., GasEOS (Reagan, 2006). As an option, users can invoke the (Redlich-Kwong) equation of state-based method in ECO2N, and these results are shown in Figure 5.4 by the symbols labeled ECO2N(RK). As shown, agreement is good over a wide range of conditions from gaseous to supercritical.

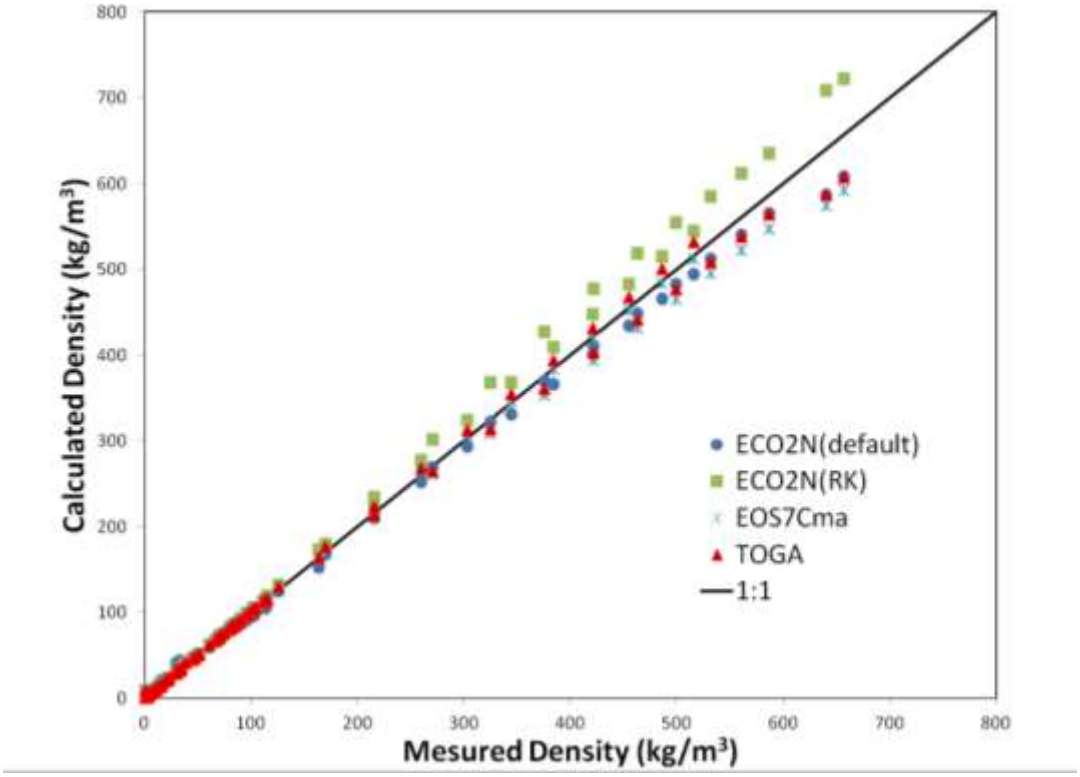

Figure 5.4. *Comparison of computed densities of the two-component (CO_2-H_2O) gas phase against the experimental data reported in the literature (Fenghour et al., 1996a & b; Patel et al., 1987; Patel and Eubank, 1988; Zawisza and Malesnska, 1981; Zakirov, 1984). The densities calculated by the other TOUGH2 EOS modules are also reported as comparison.*

Next we show enthalpy calculated in TOGA compared against ECO2N and measured data. The reference state for enthalpy is assumed to be the triple point of H_2O (P = 0.612 Pa, T = 0.01 °C).

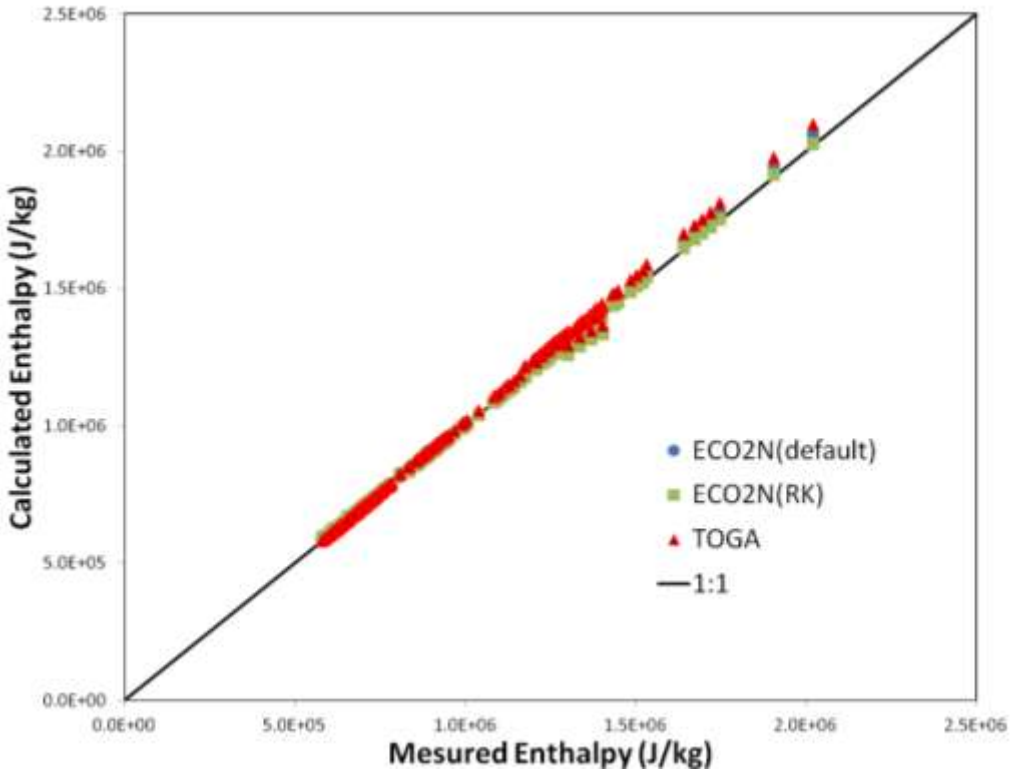

Figure 5.5. *Comparison of computed specific enthalpy of the two component (CO_2-H_2O) gas phase against experimental data reported in the literature (Patel and Eubank, 1988; Bottini and Salville, 1985; Wormald et al. 1986). The specific enthalpy values calculated by ECO2N are also reported for comparison.*

6. Verification of Flow and Transport

6.1 Introduction

In this section, we show TOGA results of flow and transport compared to results from other codes for various test problems. These verification tests serve to demonstrate that the code can correctly simulate coupled flow, transport, and phase partitioning.

6.2 Nonisothermal Radial Flow from a CO_2 Injection Well

This problem considers a radial flow geometry for which a similarity solution exists (Pruess and Spycher, 2007). In the problem, a CO_2 injection well fully penetrates a homogeneous, isotropic,

infinite-acting aquifer of 100 m thickness (Figure 6.1) at conditions of 120 bar pressure, 45˚C temperature, and aqueous phase salinity of 0 % by weight. Colder CO_2 (at 35^{o}C) is injected uniformly at a constant rate of 100 kg/s.

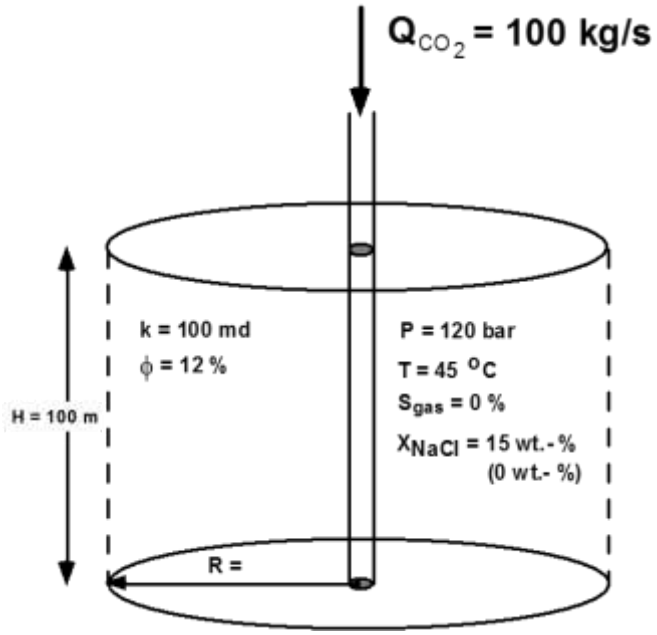

Figure 6.1. *Schematic of radial flow sample problem*

Figure 6.2 shows the comparison of the predicted pressure, temperature, and gas saturation between TOGA and two other related TOUGH modules while Figure 6.3 shows the comparison of the predicted mass fractions of CO2 in aqueous phase and H2O in gas phase. Overall, TOGA predicts similar behavior of the system as the other codes. The apparently thinner dry-out zone as shown in Fig. 6.2(b) arises because TOGA, similar to EOS7CMA, uses an evaporation model for H2O partitioning into the CO2-rich (gas) phase which results in a lower amount of water dissolving into the CO2-rich phase than the rigorous water partitioning model (Spycher and Pruess, 2005) implemented in ECO2N. This can be seen clearly in Fig. 6.3 (b). In addition,

ECO2N predicts slightly higher temperature in the “wet” side of the two phase region (Figure 6.2b) because the heat of dissolution of CO2 is accounted for in ECO2N but ignored in TOGA and EOS7CMA. The slightly higher temperature in the dry-out zone predicted by ECO2N does not occur in the TOGA and EOS7CMA results simply because the dry-out zone has not fully developed in the model by these two codes resulting in the evaporation-cooling effect persisting there.

(a)

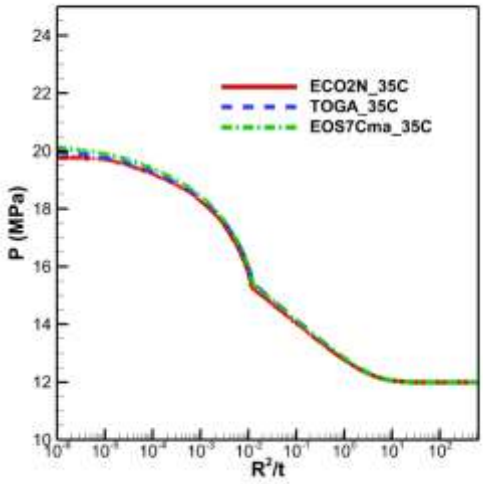

(b)

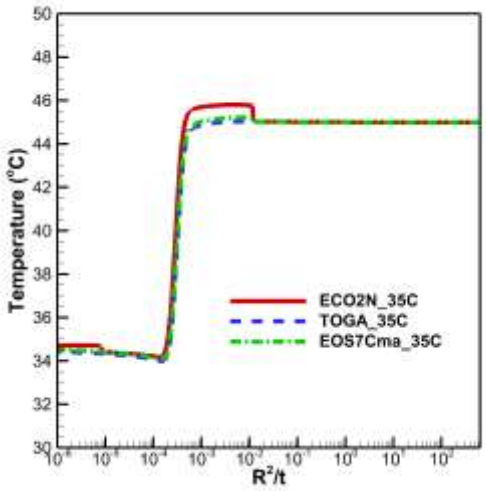

(c)

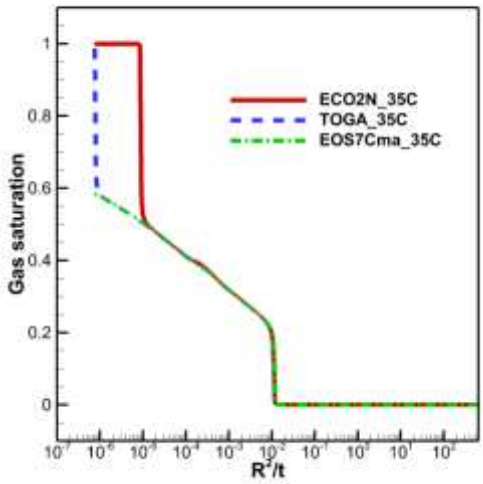

Figure 6.2. *Comparison of TOGA results against various TOUGH2 modules as a function of the similarity variable R^2/t, where R is the radius from the well and t is time. (a) simulated pressure, (b) temperature, and (c) gas saturation. The thick solid red line represents the result simulated by ECO2N, the blue dashed lines represent the result simulated by TOGA, and the green dash-dot lines represent the result simulated by EOS7CMA.*

(a) (b)

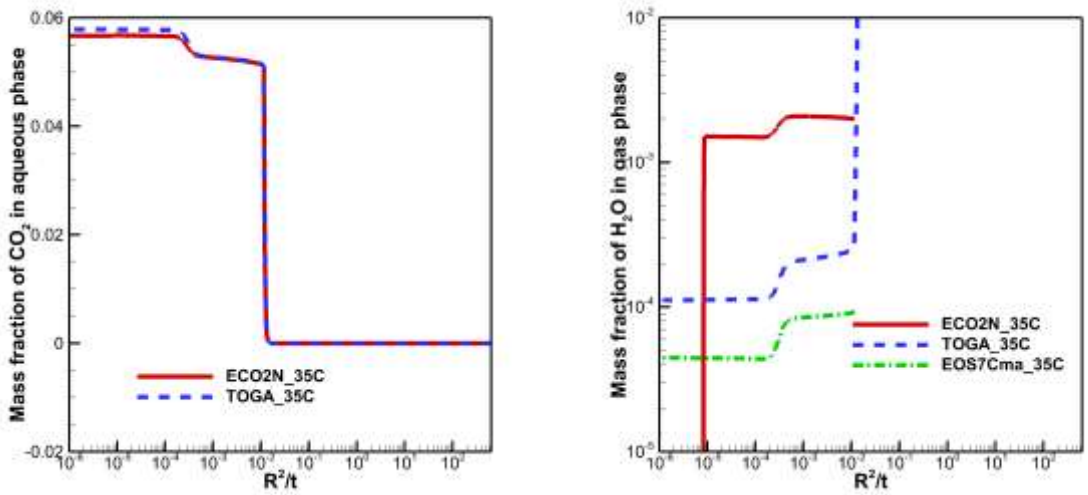

Figure 6.3. *Comparison of the simulated dissolved CO_2 mass fraction (a) and mass fraction of H_2O in gas phase (b) as a function of the similarity variable R^2/t, where R is radius from well and t is time, by various TOUGH2 modules. The thick solid red line represents the result simulated by ECO2N, the blue dash lines represent the result simulated by TOGA, and the green dash-dot lines represent the result simulated by EOS7CMA. See text for explanation.*

6.3 Simulation of 1-D three phase flow problem (comparison to CMG)

This 1-D flow problem is a problem of constant volume production from a reservoir with a size of 609.6 m × 30.48 m × 6.096 m (Figure 6.4). The reservoir is initially filled with oil (S_o = 0.8) and water (S_w = 0.2) at pressure 4002.63 psi (27.6 MPa) and temperature of 160 ^{o}C (71.1 ^{o}C). The oil composition is C1 (mole fraction = 0.5301), nC4 (0.1055), and C10 (0.3644). Five grid cells (each 60.96 m × 30.48 m × 6.096 m) are used to represent the reservoir. The detailed descriptions of the test problem and the related CMG results can be found in the Jamili (2010) dissertation.

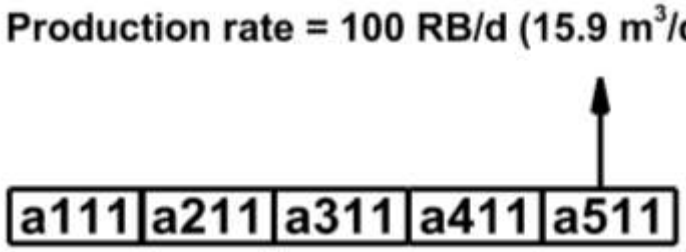

Figure 6.4. *Grid of 1-D flow problem and production rate*

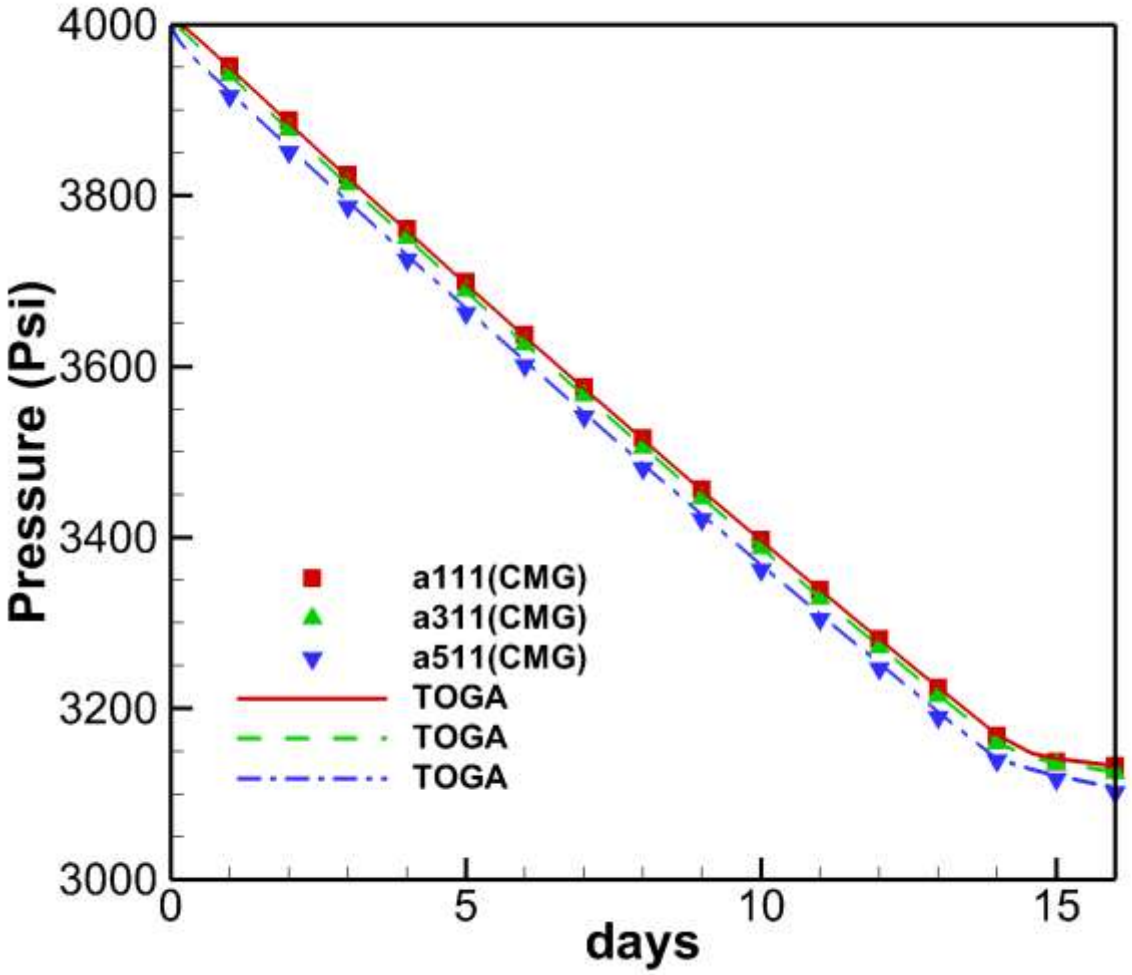

Figure 6.5. *Simulated pressure responses at selected grid cells by TOGA (lines) and CMG (symbols). Dead water (i.e., no solubility of hydrocarbon in aqueous phase nor of water in non-aqueous phase) is assumed.*

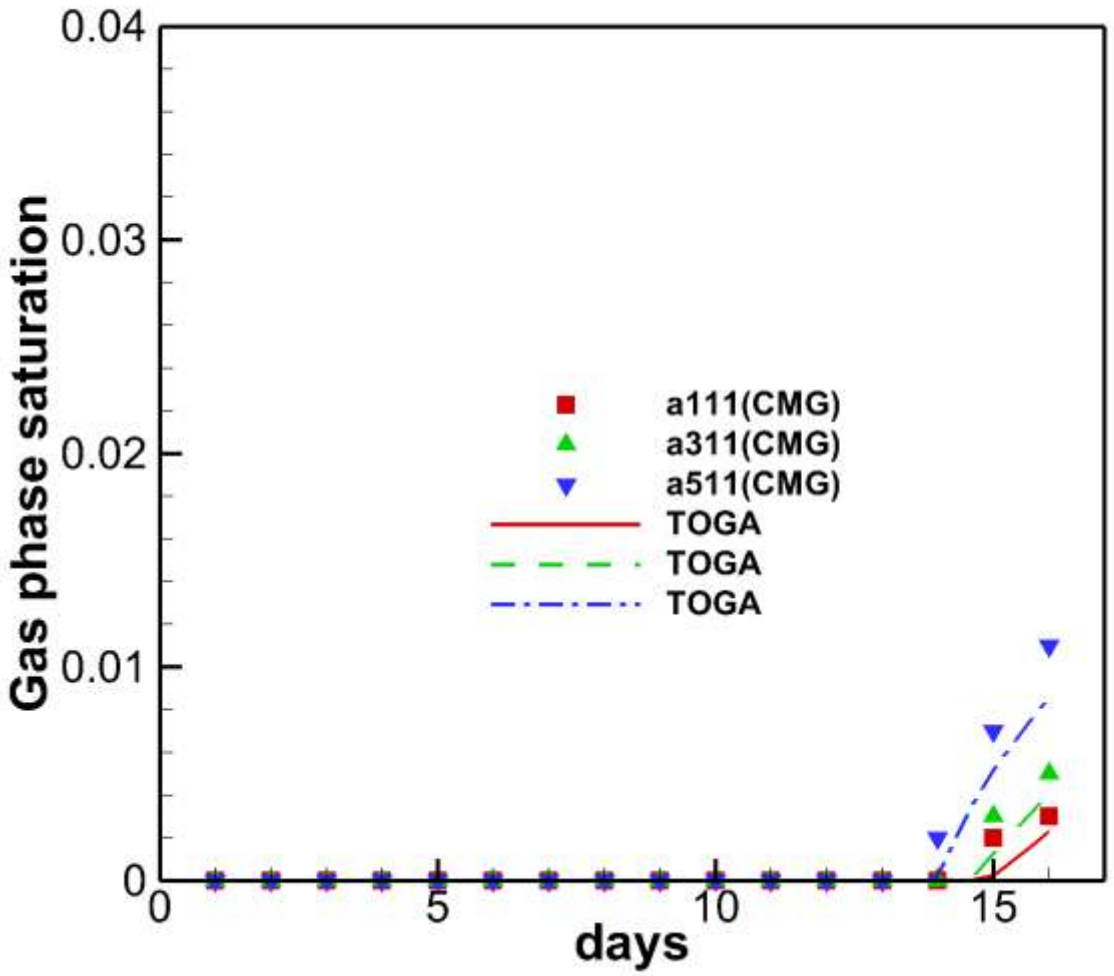

Figure 6.6. *Simulated gas saturation at selected grid cells by TOGA (lines) and CMG (symbols). Dead water (i.e., no solubility of hydrocarbon in aqueous phase nor of water in non-aqueous phase) is assumed.*

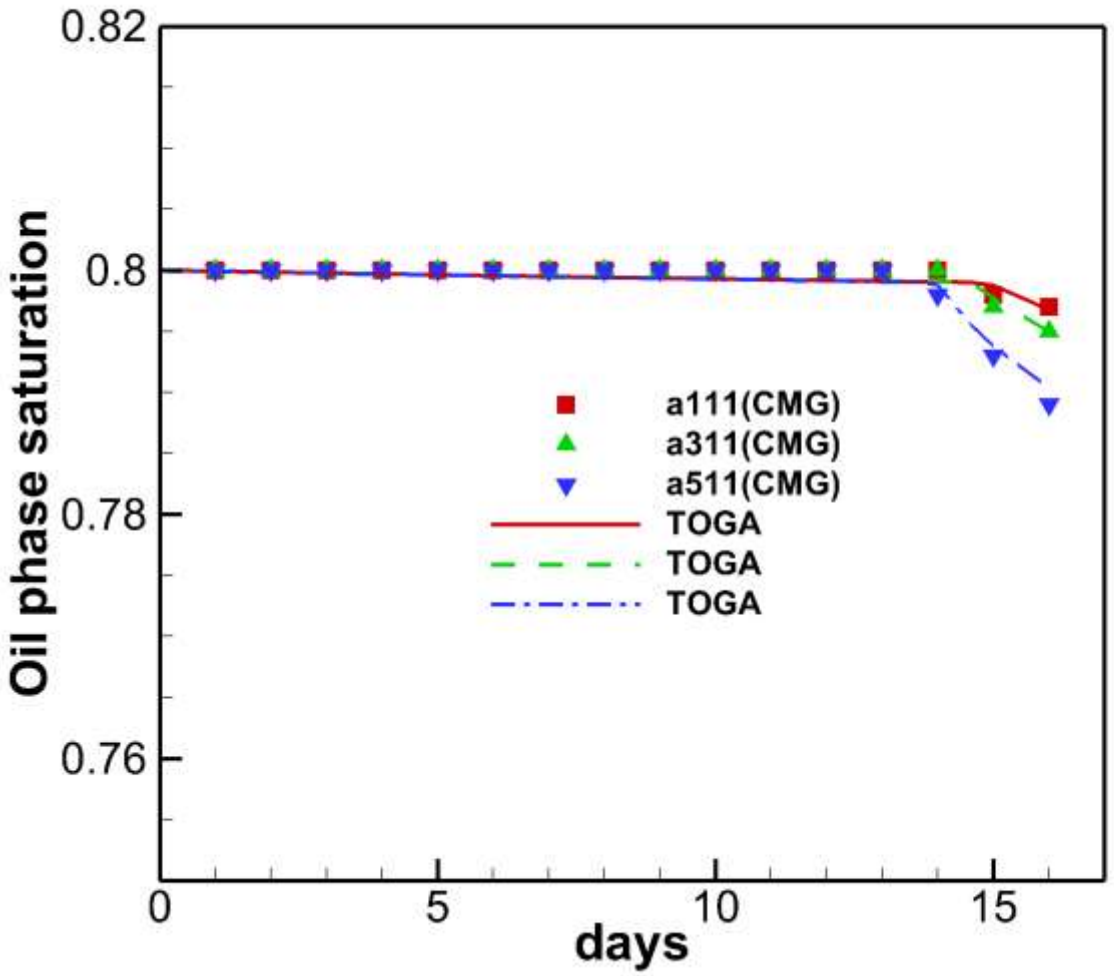

Figure 6.7. *Simulated oil saturation at selected grid cells by TOGA (lines) and CMG (symbols). Dead water (i.e., no solubility of hydrocarbon in aqueous phase nor of water in non-aqueous phase) is assumed.*

7. Validation Against One-dimensional CO_2-EOR Laboratory Experiments

7.1 Introduction

In this section, we show TOGA results compared to results from laboratory experiments of CO_2-EOR (Li et al., 2016). These validation tests serve to demonstrate that the code can correctly simulate coupled flow, transport, phase partitioning, as well as oil properties.

7.2 Oil composition and properties

The oil used in the experiment comes from HH reservoir, Shengli oil field, China. Its measured composition under reservoir conditions is shown in Table 7.1. The mole weight of heavy (C9+) component is 264.07 (g/mol). The measured bubbling pressure is 6.78 MPa and MMP is 19.9 MPa (corresponding to 90% recovery of slim tube experiment).

Table 7.1 *Composition of the test oil under reservoir conditions (65^{o}C and 20 MPa)*

Component	Mole fraction (%)
N2	2.748
CO2	0.407
C1	12.826
C2	4.139
C3	7.498
C4	5.027
C5	4.03
C6	3.69
C7	3.612
C8	3.975
C9+	52.046
Sum	100
Mole weight of C9+	264.07

Figure 7.1 shows the calculated oil density by TOGA vs. the measured oil density (Li et al., 2016) under various pressures (0.1 – 45.15 MPa) at 65 oC while Figure 7.2 shows the calculated oil viscosity by TOGA vs. the measured oil viscosity under the same conditions. The results show that TOGA can reasonably well simulate the oil density and viscosity including the degassed oil under lower pressure (e.g., 1 atm). In these calculations, the parameters of the heavy component C9+ are calibrated. These calibrated parameters are listed in Table 7.2 and will be used in following simulations of CO2 flooding experiments.

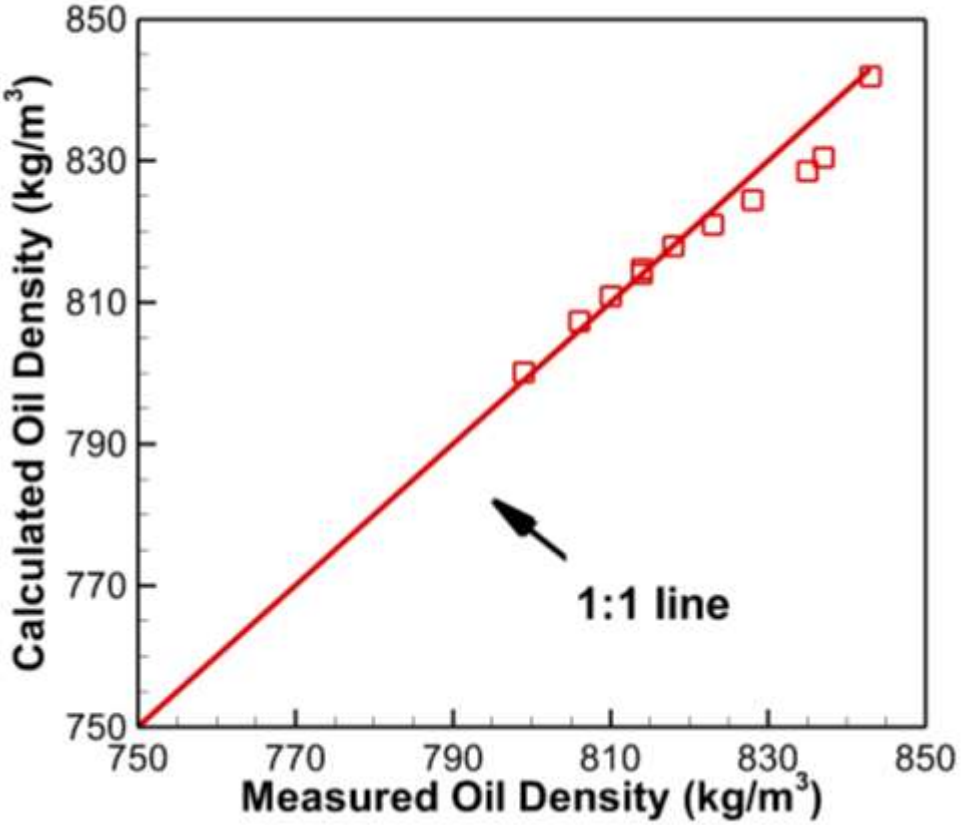

Figure 7.1 comparison of calculated oil density with the measured data

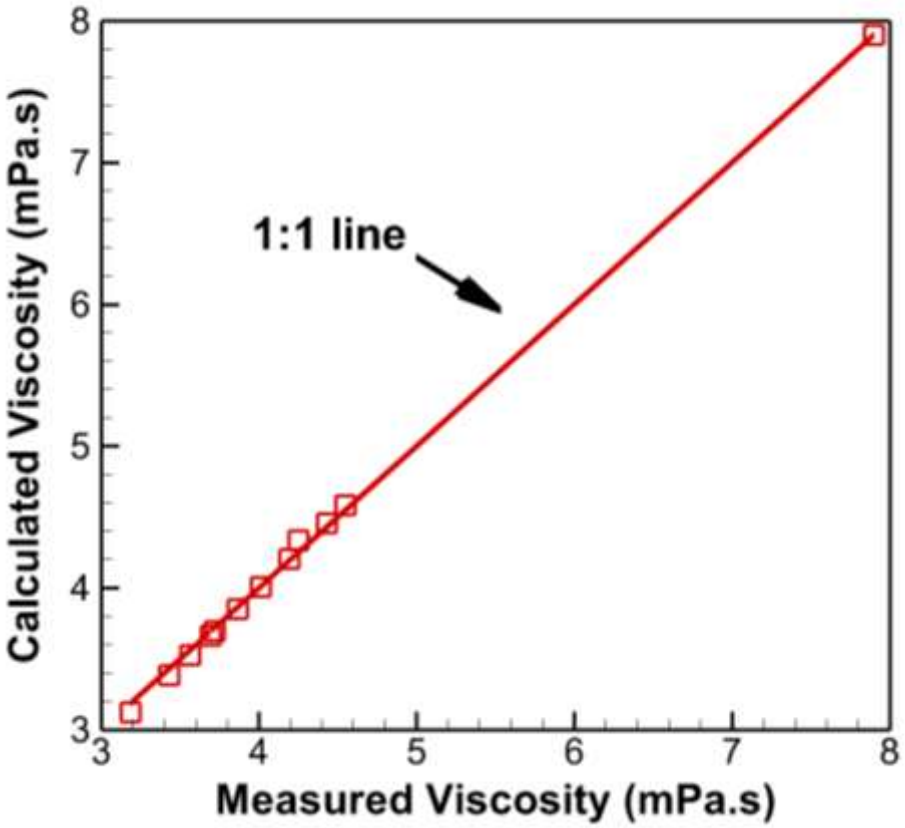

Figure 7.2 comparison of calculated oil viscosity with the measured data.

Table 7.2 Fitted parameters of the heavy components (C9+) used in the model*

Parameter	Value	Note
T_c (K)	730.00	Critical temperature
P_c (MPa)	1.6606	Critical pressure
V_c (L/mol)	1.2922	Critical volume
Z_c	0.2714	Critical compressibility
ω	0.7717	acentric factor
S_v (cm^3/mole)	-0.4646	the Penelux volume shift
d_m	0.0	Assumed to be the same as C10
μ_0	1.5010E-6	Needed to calculate viscosity of hypothetical component using (3-15)
α	1.3633E-2	
E_p	2.2990E4	
a_0	-8.3109E4	Needed to calculate the specific enthalpy at low pressure using (Eq. 3-11b); assumed to be the same as C10
a_1	1.5116E2	
a_2	2.2386E-1	
a_3	4.9350E6	

*d_m and a_0 - a_3 are not fitted in these calculations but taking the assumed values from C10. Other parameters that are not listed in this table are also taking from the internal databank by selecting the components with the closest molecular weight of the hypothetical component.

7.3 CO_2 flooding experiments

Table 7.3 shows the core geometry and basic properties of the core. Table 7.4 shows the parameters used in the simulations of two scenarios, immiscible and miscible CO_2 flooding. The EOR experiments are simulated as one-dimensional isothermal flow with a fixed injection of pure CO_2 at one end and a constant back-pressure at the other end of a horizontal core. The STONE II model is used for three-phase relative permeability with two-phase relative permeabilities shown in Figures 7.3 and 7.4 (Water-oil and Gas-oil, respectively). The oil capillary pressure is adjusted by the local oil-gas interfacial tension in the simulations. The curves in Fig. 7.3 and 7.4 are scaled by the measured Swc for each case (immiscible or miscible).

Table 7.3 Properties of the long composite rock core used in the experiments.

Parameter	Value	Note
Total length (cm)	32.904	
Diameter (cm)	2.53	
Number of sections	6	Arranged from higher to lower i
Average porosity (%)	9.928	Water weighting method
Permeability of the assembled core (md)	0.06319	Measured at 20^{o}C with water sat
Swc (%)	42.43 – 44.56	Measured by oil flooding the wa
Oil permeability at Swc (md)	0.0275-0.0278	until no water produced. Differe gives slightly different values

Table 7.4 Model set up of the simulations

Parameter		Value	Note
Number of grid cells		12+2	Two additional grid cells are boundary cells atta outlet of the core
T (^{o}C)		65.0	Reported reservoir temperature
Immiscible	P_{ini} (Mpa)	8.00	
	So_{ini} (%)	57.57	
	P_{back} (Mpa)	8.57	Average measured back pressure

	CO_2 injection rate (kg/s)	2.0e-7	Fitted value. Original experiment setting is 0.1 n density.
Miscible	P_{ini} (Mpa)	20.00	
	So_{ini} (%)	55.44	
	P_{back} (Mpa)	20.45	Average measured back pressure
	CO_2 injection rate (kg/s)	2.8e-7	Fitted value. Original experiment setting is 0.1 n density.

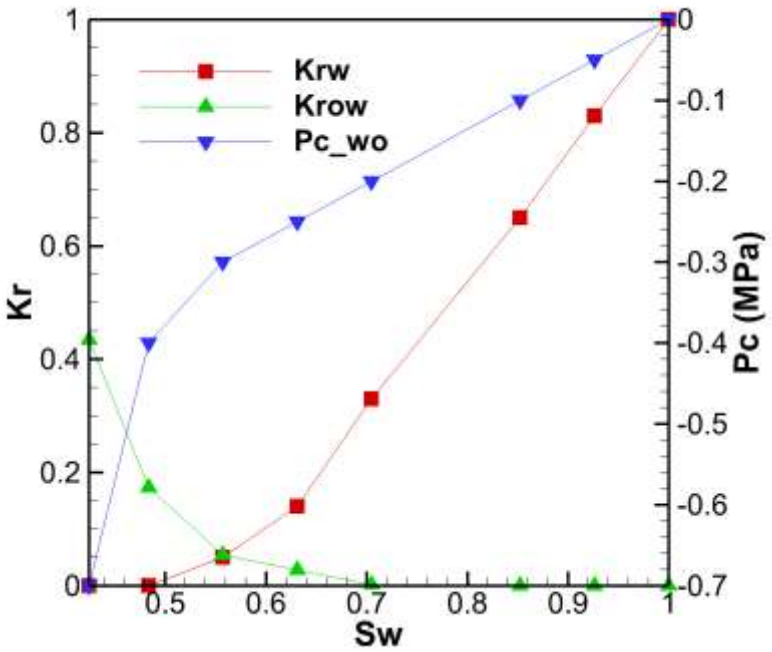

Figure 7.3 The relative permeability and capillary pressure curves of water-oil system

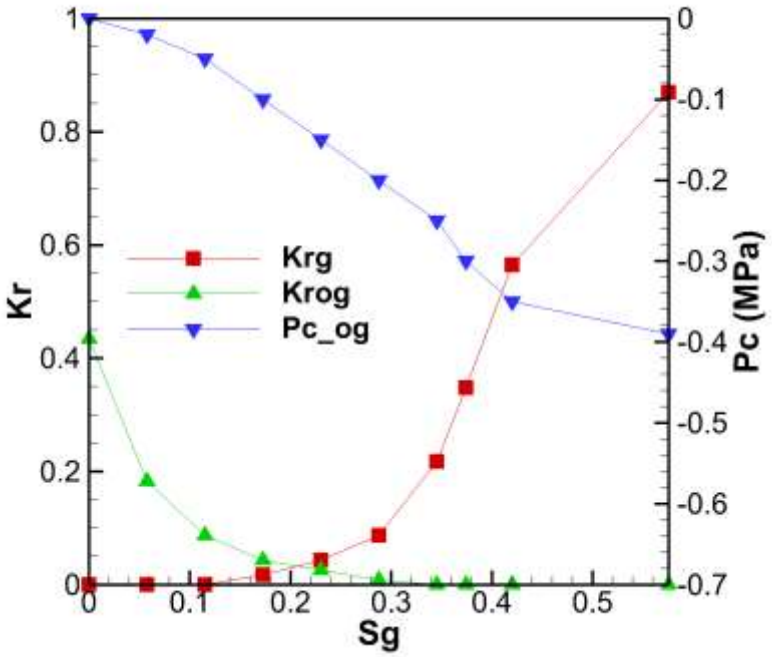

Figure 7.4 The relative permeability and capillary pressure curves of gas-oil system under connated water saturation

As shown in Figure 7.5, TOGA can reproduce the production volumes reasonably well even though the heterogeneity of the core is ignored. The effects of displacement pressure on the production of oil are obvious. For pressures above MMP (minimum miscibility pressure), more oil can be produced and the gas (CO_2-rich) phase breakthrough occurs later. Figure 7.6 shows the comparison of the calculated pressure difference between the inlet and the outlet of the core against the measured values. TOGA captured the major trend of the variations in the pressure difference reasonably well considering that the simple 1D uniform model does not include all of the details of the compositional core experiments.

(a) (b)

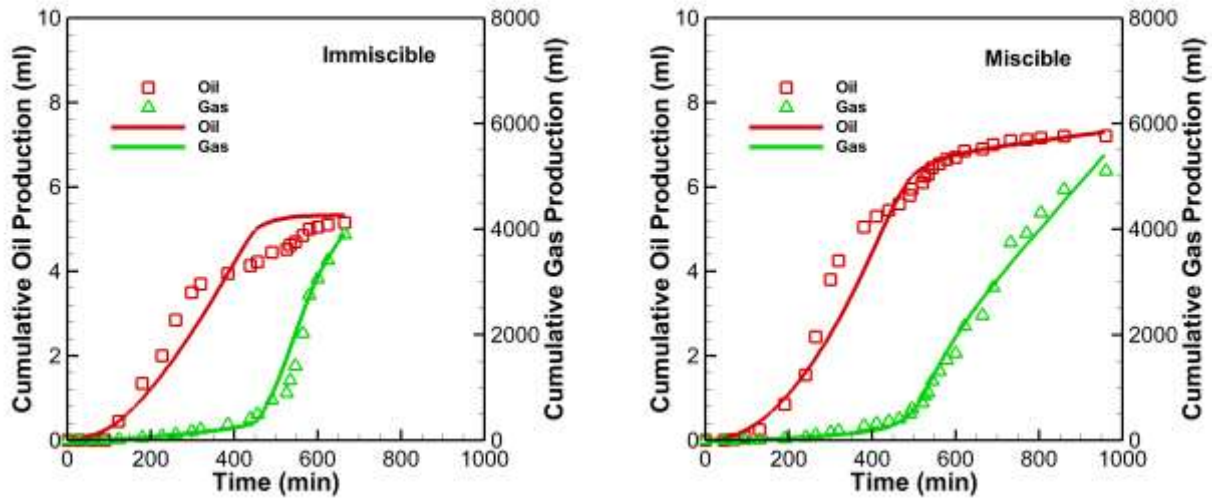

Figure 7.5 Simulated (solid lines) and measured (symbols) oil and gas production: (a) immiscible flooding (back-pressure = 8.57 MPa) and (b) miscible flooding (back-pressure = 20.45 MPa). The cumulative production volumes are calculated at P = 1 atm and T = 65°C.

(a) (b)

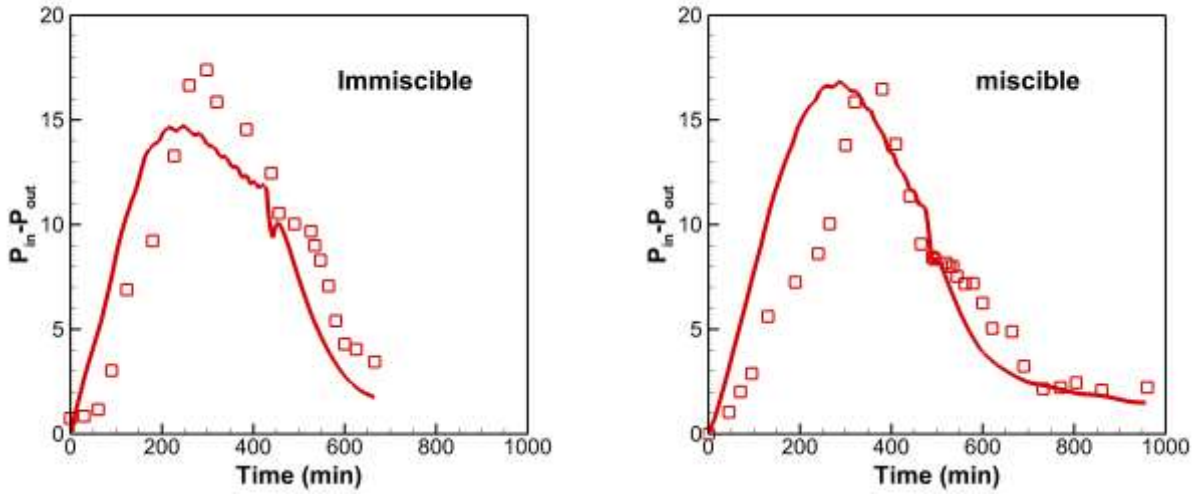

Figure 7.6 Simulated (solid lines) and measured (symbols) pressure difference between inlet and out let of the core during CO_2 flooding experiment: (a) immiscible flooding (back-pressure = 8.57 MPa) and (b) miscible flooding (back-pressure = 20.45 Mpa).

8. Three-Dimensional Examples

8.1 Introduction

In this section, we will demonstrate an application of TOGA for simulating CO_2-EOR processes in a 3D reservoir.

8.2 Conceptual model and grid

The oil reservoir we consider here is an idealized 50 m-thick porous reservoir. One injection well/production well pair is modeled as part of a five-spot well configuration with a basic pattern area of 1 km^2 (Fig. 8.1), as was considered in Pruess (2006). Because of the areal symmetry, only 1/8 of the basic pattern area (and also 1/8 of the injection and production rates) needs to be modeled, with no-flow boundaries on all sides. A three-dimensional (3D), five-layer irregular grid was created to represent the reservoir (Fig. 8.2). Grid-block size varies from 0.5 m near the wells to 25 m in the far field to capture the important details of the flow field. Both the injection and production wells have a diameter of 0.5 m and fully perforate the reservoir. One additional grid cell is attached to the top of each well to facilitate the assignment of boundary conditions. A very large volume is assigned to the cell attached to the top of the production well (Figure 8.3). The connections between these additional boundary grid blocks and the related well grid blocks are defined as one-way connections (Figure 8.4). TOGA will output the cumulative gas and oil volumes at the standard conditions through these special connections to the COFT file if these connections are listed in the COFT section of the input file. The standard conditions (*P* and *T*) are specified using a keyword PROPT. Figure 8.5 shows an example of how to assign the standard conditions in the input file but note that we use 15.0 ºC for this example.

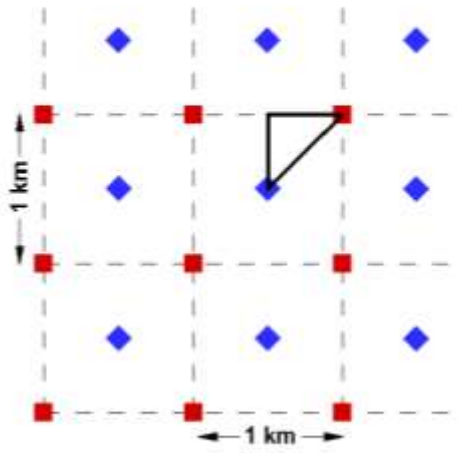

Figure 8.1 Diagram of five-spot pattern of geothermal wells (blue-injector; red-producer) showing the triangular one-eighth symmetry element.

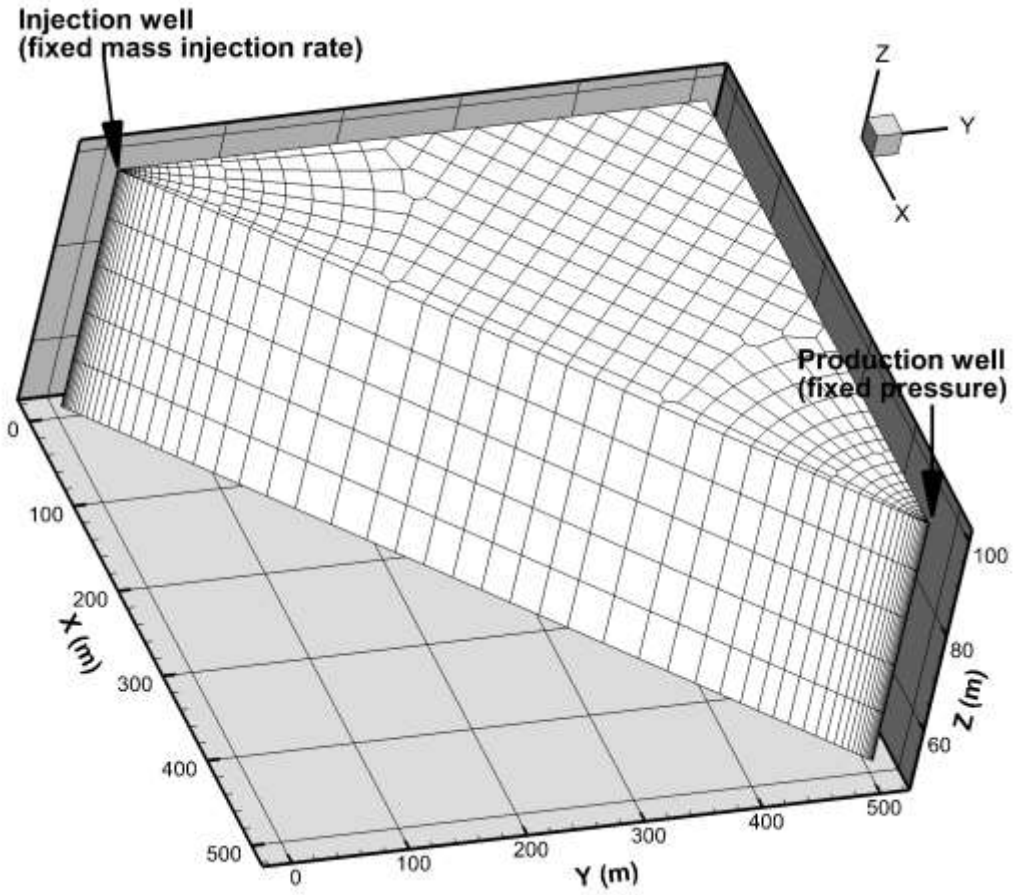

Figure 8.2 The numerical grid used in the simulation. Finer grid resolution is used near the two wells.

```
ELEME
0AC58          wella2.7300E+000.0000E-020.0000E+001.0000E-021.0000E-02   100.000
0AD43          wella2.4600E+510.0000E-020.0000E+00   500.000   500.000   100.000
1AA 1          Rock14.2600E+034.2600E+020.0000E+00   178.033   180.546    95.000
1BA 1          Rock14.2600E+030.0000E+000.0000E+00   178.033   180.546    85.000
1CA 1          Rock14.2600E+030.0000E+000.0000E+00   178.033   180.546    75.000
… …
```

Figure 8.3. The special grid block ('0AD43') for assignment of constant pressure with large volume (highlighted) in the input file.

```
CONNE
1AC580AC58                    45.0000E+001.0000E-152.7300E-02-1.000E+00
0AD431AD43                    41.0000E+001.0000E-002.7300E-01 0.000E+00
1BA 11AA 1                    35.0000E+005.0000E+004.2600E+02-1.000E+00
1CA 11BA 1                    35.0000E+005.0000E+004.2600E+02-1.000E+00
```

Figure 8.4. One-way connections in the input file. The flow is allowed only from C2 ('0AC58' or '1AD43') to C1 ('1AC58' or '0AD43') if ISO is set to be 4 (highlighted). Similarly, the flow is allowed from C1 to C2 if ISO is set to be 5. The parameter (ISO > 3) also serves a flag to let TOGA output the cumulative oil and gas phase volumes at the user-specified standard conditions through the connection in the COFT output file if the connection is in the output list.

```
PROPT
1.0135e5
65.0
```

Figure 8.5. Assignment of standard conditions for output of gas and oil volume. The first value is the standard pressure (Pa) and the second value is the standard temperature (^oC). The default standard P and T are 1.0135e5 Pa and 15.0 ^oC, respectively, if they are not specified in the input file.

8.3 Rock properties

The formation consists of a single uniform rock with lower permeability in the vertical direction (Table 8.1). We approximate the well as an equivalent porous medium with high permeability and no capillary. The tabular data input of relative permeability and capillary pressure are shown in Figure 8.6.

Table 8.1 Parameters of formation and wellbore

Parameter	Formation	Wellbore
Horizontal Permeability k_x, k_y (m^2)	10^{-12}	10^{-8}
Vertical Permeability k_z (m^2)	0.2×10^{-12}	10^{-8}
Porosity, ϕ	0.2	0.5
Pore compressibility (Pa^{-1})	10^{-9}	0
Relative permeability:	STONE II (IRP=15)	Power function (IRP=11)
Residual gas saturation	Tabular data (see Figure 8.6)	0.01
Residual oil saturation		0.01
Residual liquid saturation		0.01
Power		1.0
Parameters for capillary pressure:	Tabular data (see Figure 8.6)	No capillary (ICP=9)

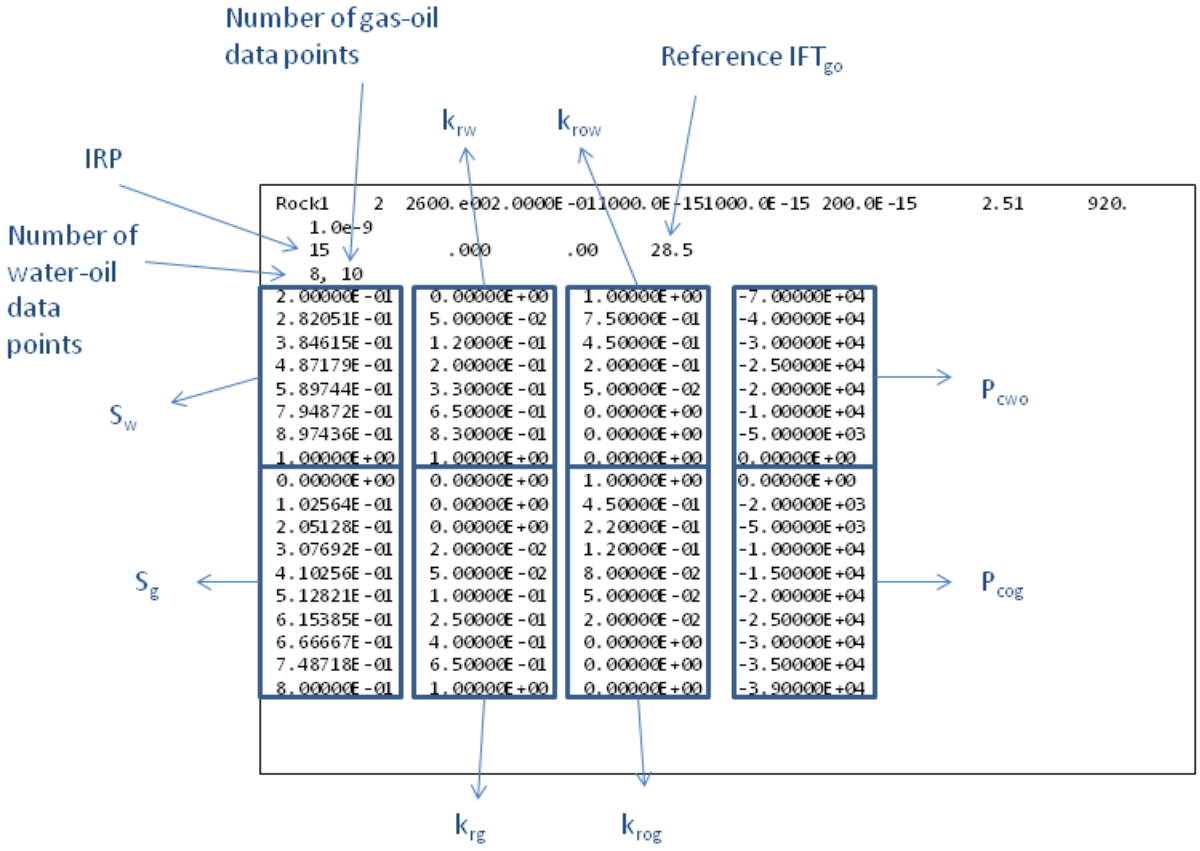

Figure 8.6. The relative permeability and capillary pressure data tables and other related parameters for the STONE II model as used in the TOGA input file.

8.4 Oil composition and properties

The oil composition in the reservoir is assumed to be the same as that in the HH reservoir (Table 7.1). The oil properties are also described in Section 7.2. Figure 8.7 shows the composition definition and parameters of the hypothetical component (C9+) in TOGA input file.

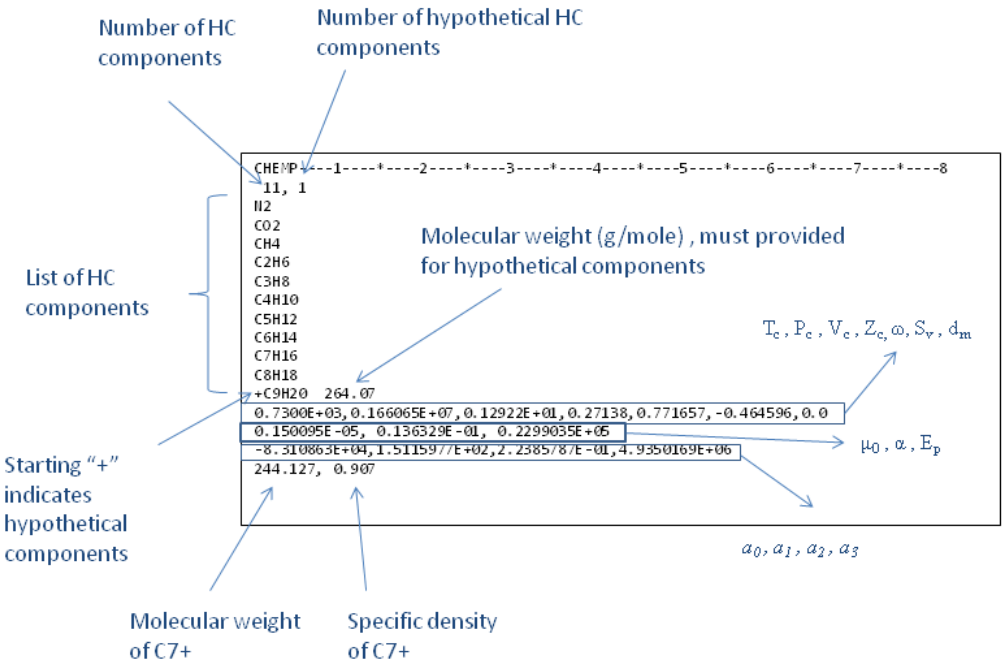

Figure 8.7. Input of 'CHEMP' section defining the composition of oil in the reservoir. If a component is not in the internal data bank, it must be defined as a hypothetical component (i.e., the first character of the component name must be '+') and its molecular weight (g/mol) must be provided (real number after column 8). Three rows of additional parameters for the component must also be provided right below that component. If there are multiple hypothetical components, the inputs are repeat in the same manner. The last two entries of 'CHEMP' section are the molecular weight (g/mol) and the specific density of C7+ components which is needed in the calculation of equilibrium coefficient using the empirical K-value method.

8.5 Initial and boundary conditions

The reservoir is assumed to be initially filled with mostly oil and some water under equilibrium pressure. In the immiscible case, the pressure is slightly above 8 MPa (Figure 8.8) whereas the pressure is slightly above 20 MPa (Figure 8.9) in the miscible case. The temperature is 65oC for both cases and simulations are all isothermal. No gas phase exists initially in both cases.

No flow boundary is assumed for all sides of the domain except at the top of the production well where a fixed back pressure is assigned with a value of 8 MPa for the immiscible case and 20 MPa for the miscible case, respectively. Pure CO2 is injected at a rate of 3.125 kg/s (25 kg/s for the full well) through the top of the injection well for both cases.

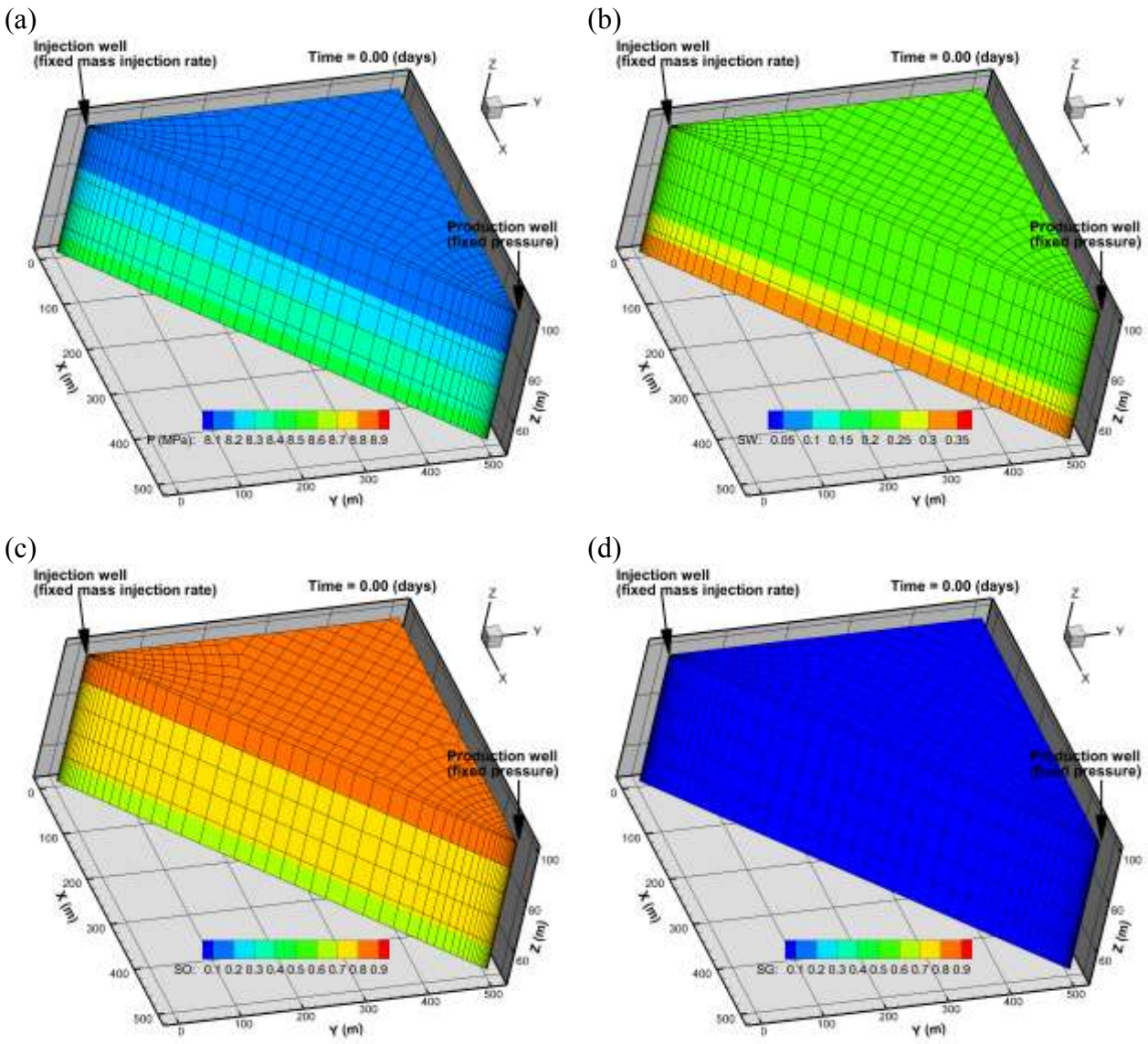

Figure 8.8 Initial pressure (a), water saturation (b), oil saturation (c), and gas saturation (d) in the reservoir of the immiscible CO_2 flooding case.

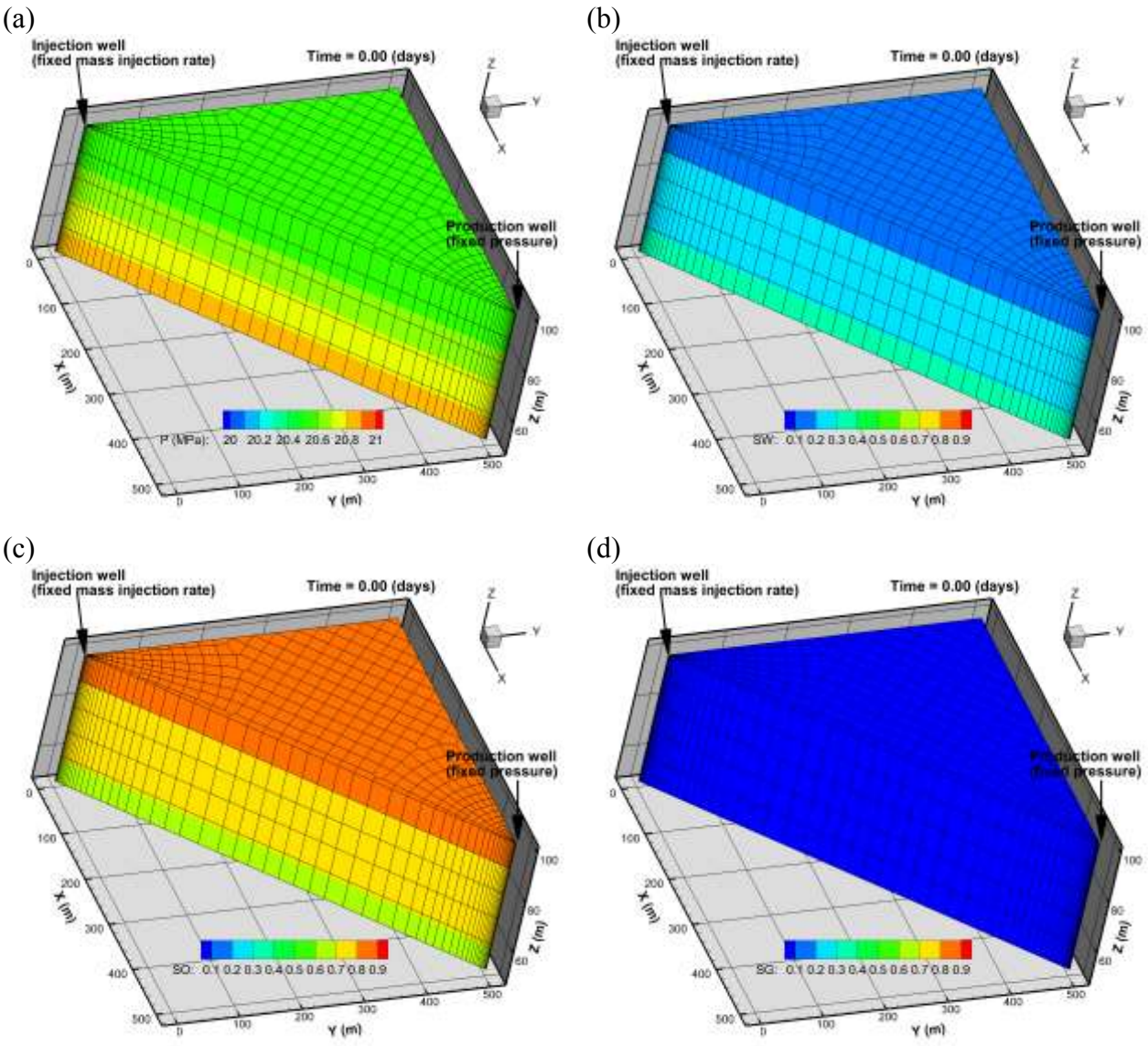

Figure 8.9 Initial pressure (a), water saturation (b), oil saturation (c), and gas saturation (d) in the reservoir of the miscible CO_2 flooding case.

8.6 Results

Figure 8.10 shows the flow rates and cumulative production volumes as they respond to the continuous injection of CO2 under miscible and immiscible conditions. Under miscible

conditions, the production of both oil and water increases quickly to a stabilized level as a result of the pressurization of the reservoir due to CO2 injection at early time (Figure 8.10 a). This stable production period ends at about 400 days when the oil production starts to increase associated with decreasing production of water. The increasing trend of oil production turns around to become a decreasing trend at about 1300 days (~3.56 yrs), about two months before the gas phase breakthrough. After breakthrough of gas phase at the production well, the production of oil quickly decreases. This process can also be seen in the cumulative volumes (Figure 8.10 b). The production of oil is almost proportional to the injection of CO2 for the first couple of years. As most of the mobile water is removed, the oil production rate increases significantly. However, when the gas phase breaks through to the production well, the cumulative oil production volume starts to flatten out.

(a) (b)

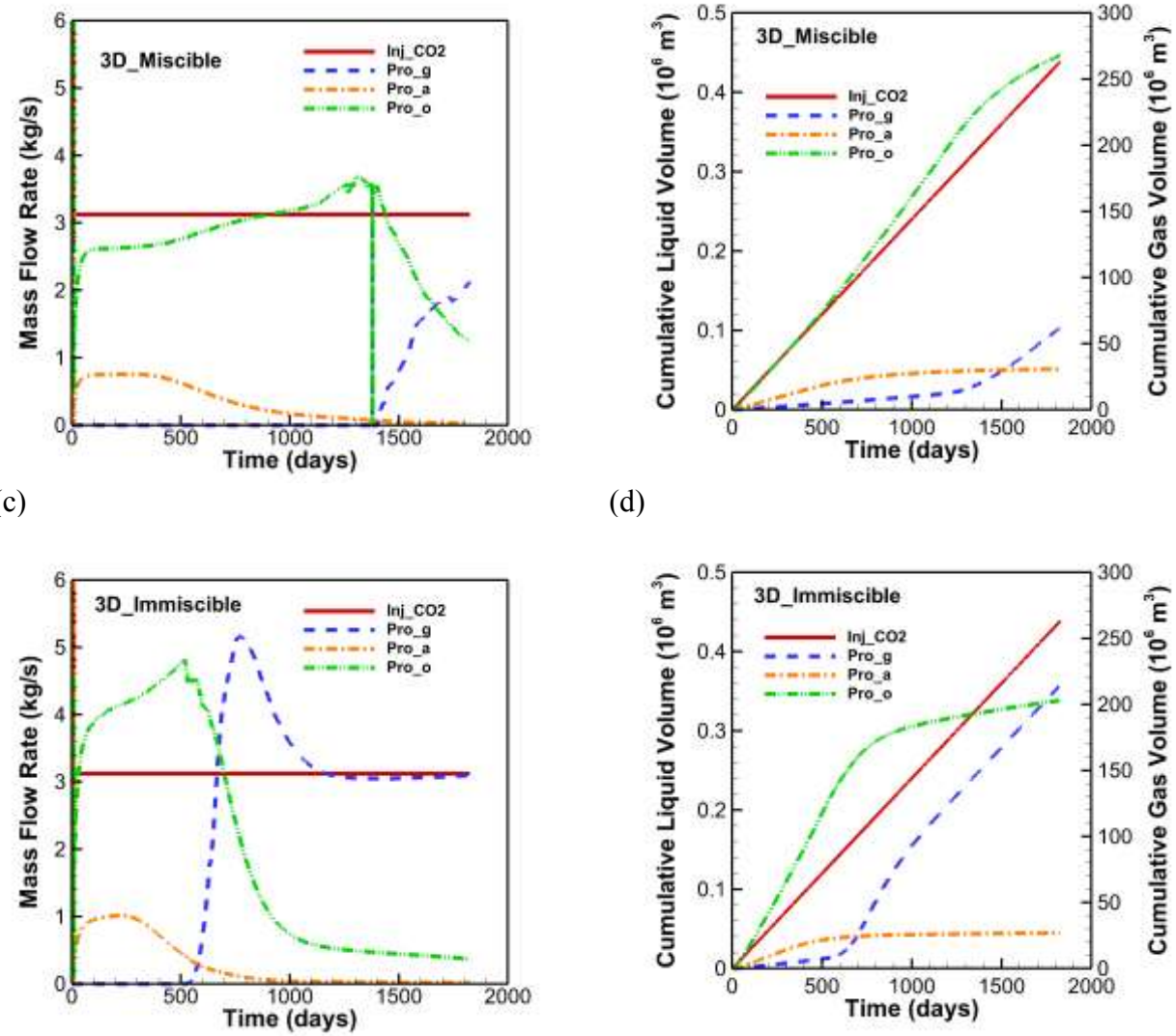

(c) (d)

Figure 8.10. Simulated production responding to continuous CO_2 injection: (a) the mass flow rate (kg/s), miscible; (b) the cumulative injection/production volume (at P = 1 atm and T =15°C), miscible; (c) the mass flow rate (kg/s), immiscible; and (d) the cumulative injection/production volume (at P = 1 atm and T =15°C), immiscible . "Inj_CO2" – injection of CO_2 at the injection well; "Pro_g" – production of gas; "Pro_a" – production of water; and "Pro_o" – production of oil. All values are for 1/8 of wells. In (b), water and oil are plotted on the left-hand vertical axis while gas and CO_2 are plotted using the right-hand vertical axis.

Under immiscible conditions, the patterns are similar but the period of the first stabilized production of oil and water is much shorter with significantly higher rates (Figure 8.10c). the oil

production starts to drop quickly at about 500 days when the gas phase breakthrough the production well. The gas production rate finally reduces to the level of the injection after a peak as gas phase flow becomes the dominant flow. In terms of cumulative production volume (at standard conditions), the immiscible conditions tend to produce more oil at early time but significant less in total 5 years of CO2 flooding (Figure 8.10d) then the miscible conditions (Figure 8.10b). Producing more oil at early time is because more volume is injected for the same mass of CO2 under the immiscible conditions (lower pressure) than under the miscible conditions (higher pressure). Less in total oil production is because the much earlier breakthrough of gas phase due to less miscibility between CO2 and oil under the immiscible conditions.

As shown in Table 8.2, under the miscible conditions, the reservoir stores about 3 times of CO2 as that under the immiscible conditions after 5 years of injection. Meanwhile, the residual oil (represented as C4+) in the reservoir is 65×106 kg less under the miscible conditions than the immiscible conditions. About 53% of oil (represented by C4+) initially in the reservoir is produced at end of 5 years of CO2 injection under the miscible conditions (Figure 8.11) but this number is only 41% for the immiscible case.

Table 8.2 Mass of CO_2 and C4+ components in reservoir

	CO2 (10^6 kg)		C4+(10^6 kg)	
Time	immiscible	miscible	immiscible	miscible
0 day	0.94	0.96	712.16	721.13
10 days	3.64	3.65	711.38	720.36
100 days	27.90	27.93	686.62	703.07
0.5 yr	50.18	50.22	659.87	685.59
1.0 yr	99.41	99.48	597.51	646.61
1.5 yrs	148.40	148.74	529.91	606.32
2.0 yrs	158.61	197.99	479.66	563.35

2.5 yrs	131.90	247.24	456.47	518.00
3.0 yrs	124.88	296.46	445.87	471.03
3.5 yrs	125.26	343.40	438.17	422.85
4.0 yrs	126.61	375.67	431.34	386.25
5.0 yrs	127.80	396.30	425.07	360.85

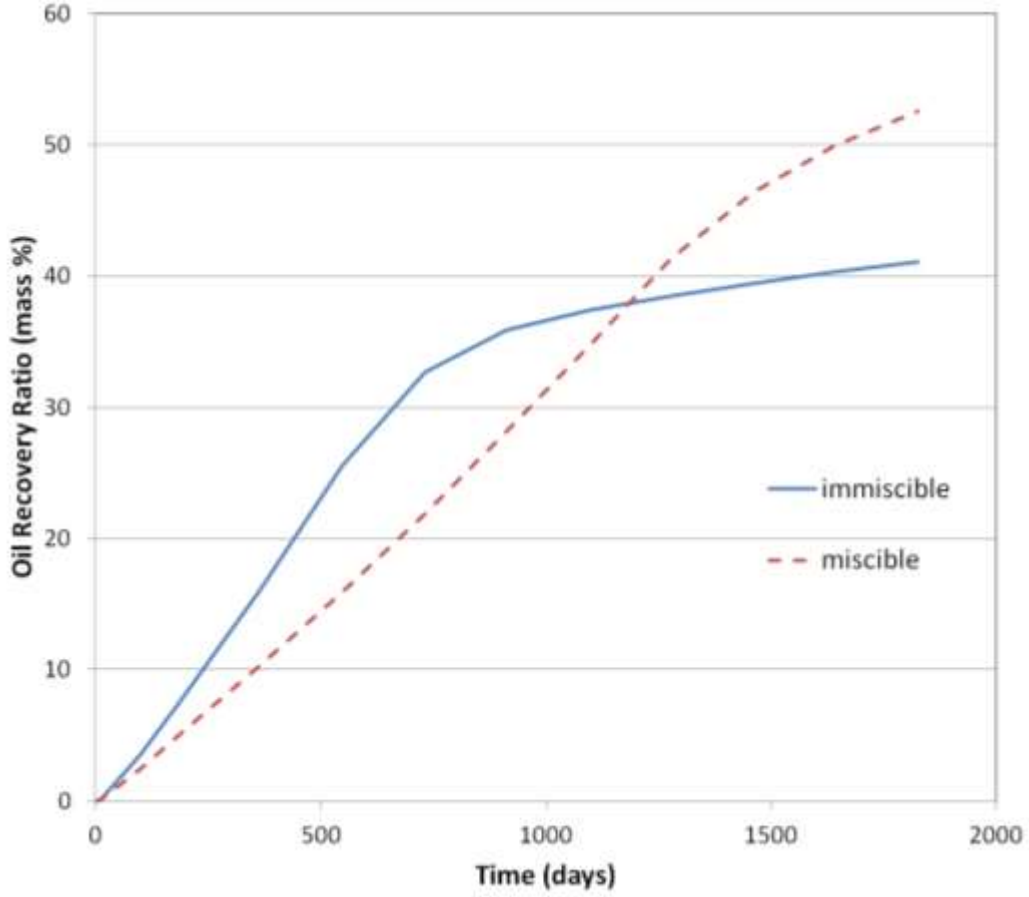

Figure 8.11 simulated oil recovery (mass) ratio for the miscible and the immiscible cases

Figure 8.12 shows the distribution of reservoir pressure during CO_2 injection under immiscible conditions. Both the reservoir pressure and the pressure gradient are larger at early time (e.g., 100 days and 1 year) than at later time because of the significant decrease in flow resistance due to breakthrough of gas (CO_2-rich) phase. The CO_2 breakthrough takes place at the upper portions of the formation (Figure 8.13). The change in oil saturation is small after breakthrough of CO_2

(Figure 8.14 c, d, e, and f), indicating low sweeping efficiency. This significant pressure drop in the reservoir occurs much later under miscible conditions (Figure 8.15) because CO_2 breakthrough takes place much later (after 3 years of injection instead of 1.5 years) as shown in Figure 8.16. Figure 8.17 shows the corresponding distribution of oil phase in the reservoir. Figure 8.18 shows the evolution of water saturation in the reservoir under immiscible flooding conditions whereas Figure 8.19 shows water saturation under miscible flooding conditions. In both cases, the water saturation is approaching the residual saturation in most areas after 1 year of injection except for the region around the injection well where the formation is dried out because the residual water is removed by evaporation into the flowing CO_2.

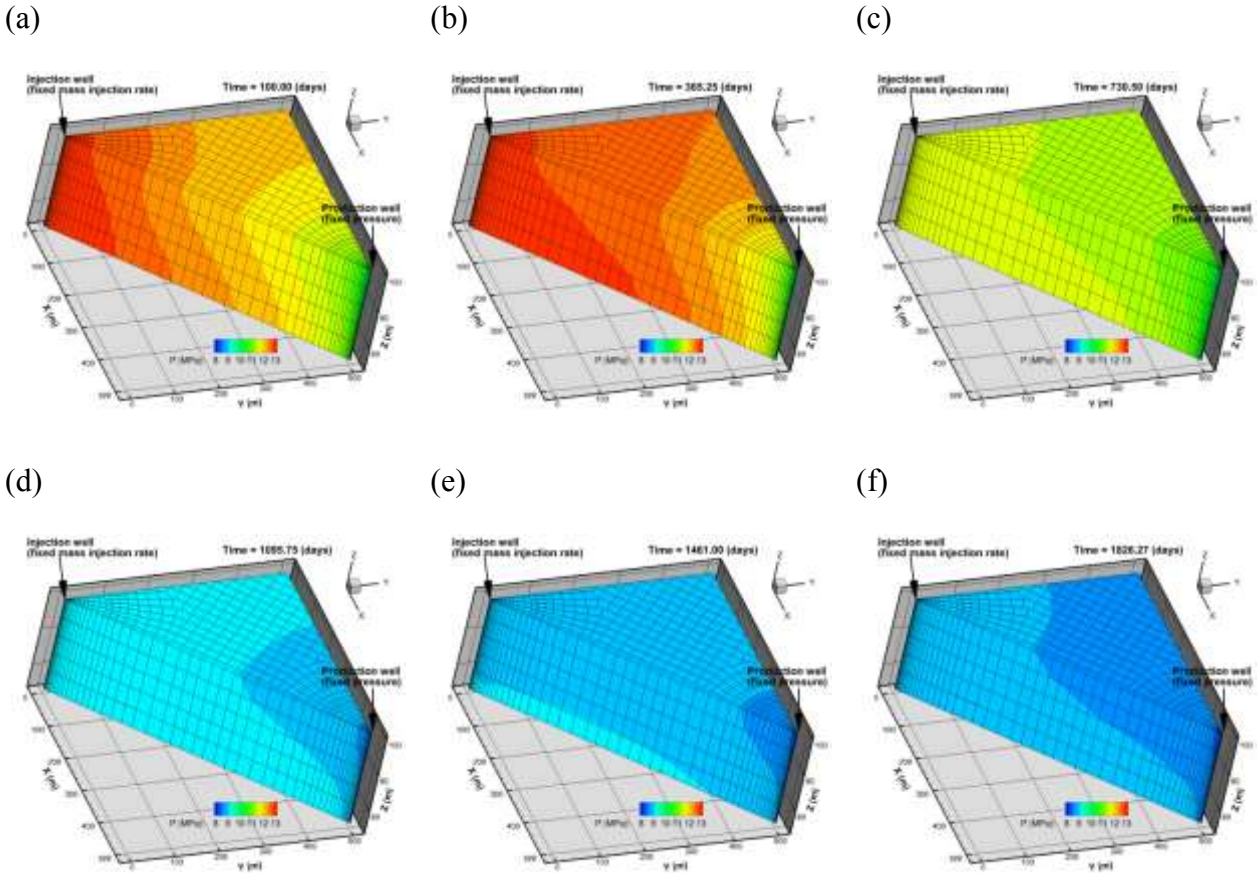

Figure 8.12. Simulated reservoir pressure distribution under immiscible conditions at various times, (a) 100 days, (b) 1year, (c) 2 years, (d) 3 years, (e) 4 years, and (d) 5 years.

(a) (b) (c)

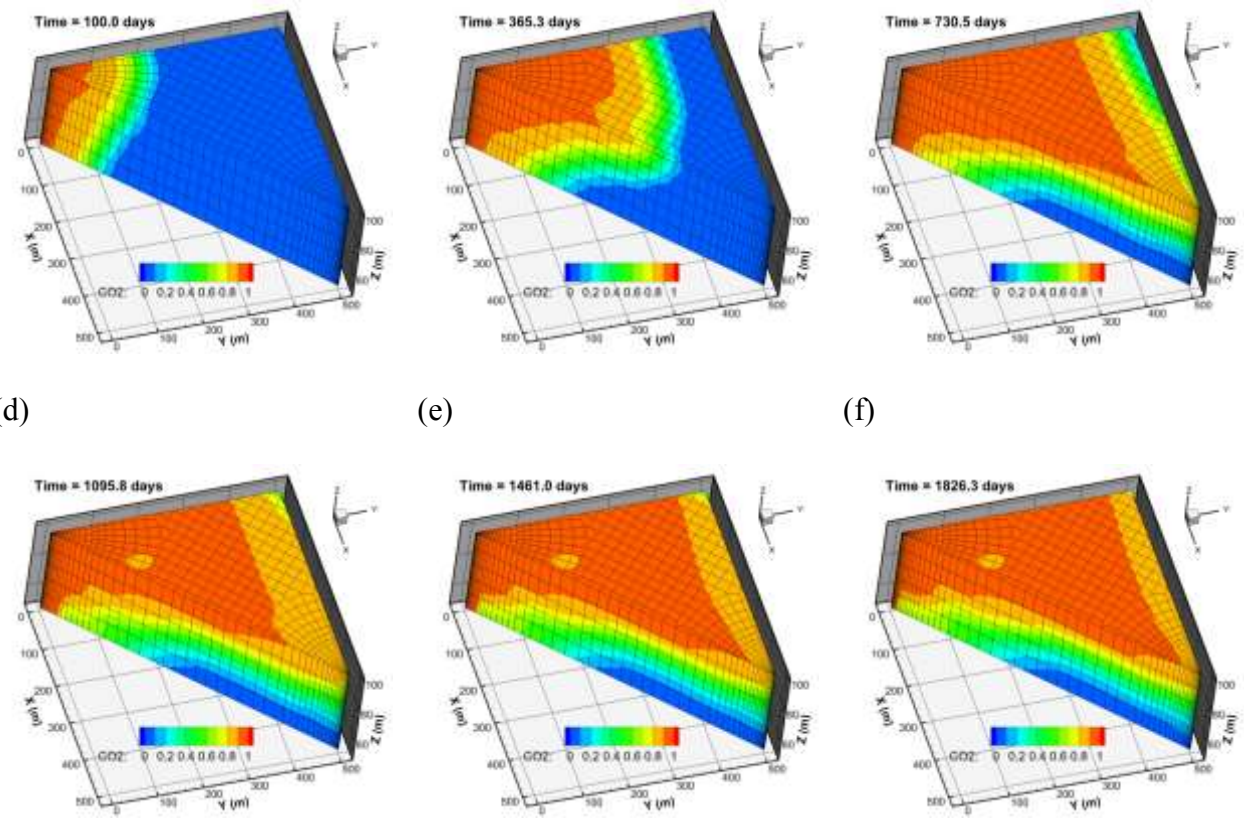

(d) (e) (f)

Figure 8.13. Calculated CO_2 mole fractions in the HC components (primary variables) under immiscible conditions, (a) 100 days, b) 1 year, (c) 2 years, (d) 3 years, (e) 4 years, and (d) 5 years.

(a) (b) (c)

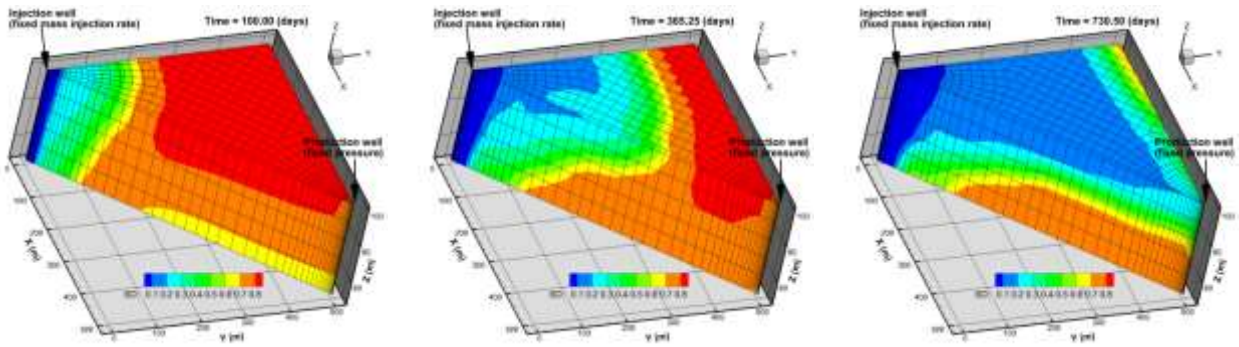

(d) (e) (f)

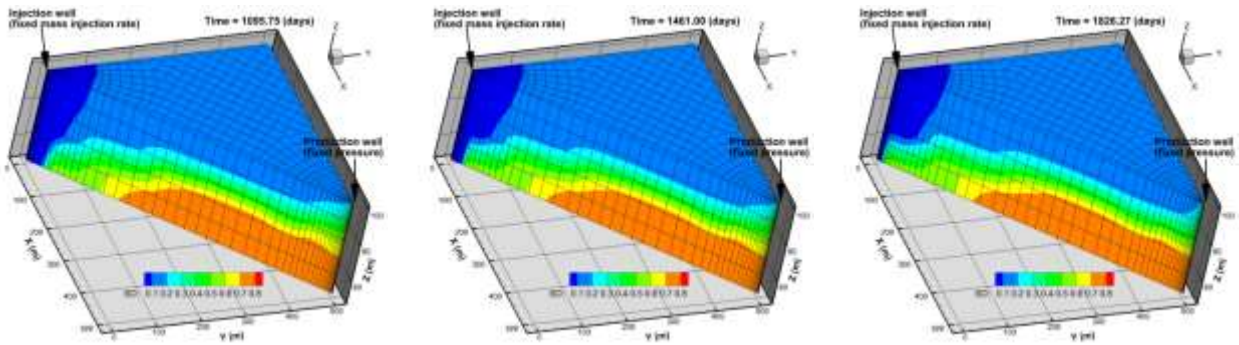

Figure 8.14. Calculated oil saturation in the reservoir under immiscible conditions at various times, (a) 100 days, (b) 1year, (c) 2 years, (d) 3 years, (e) 4 years, and (f) 5 years.

(a) (b) (c)

(d) (e) (f)

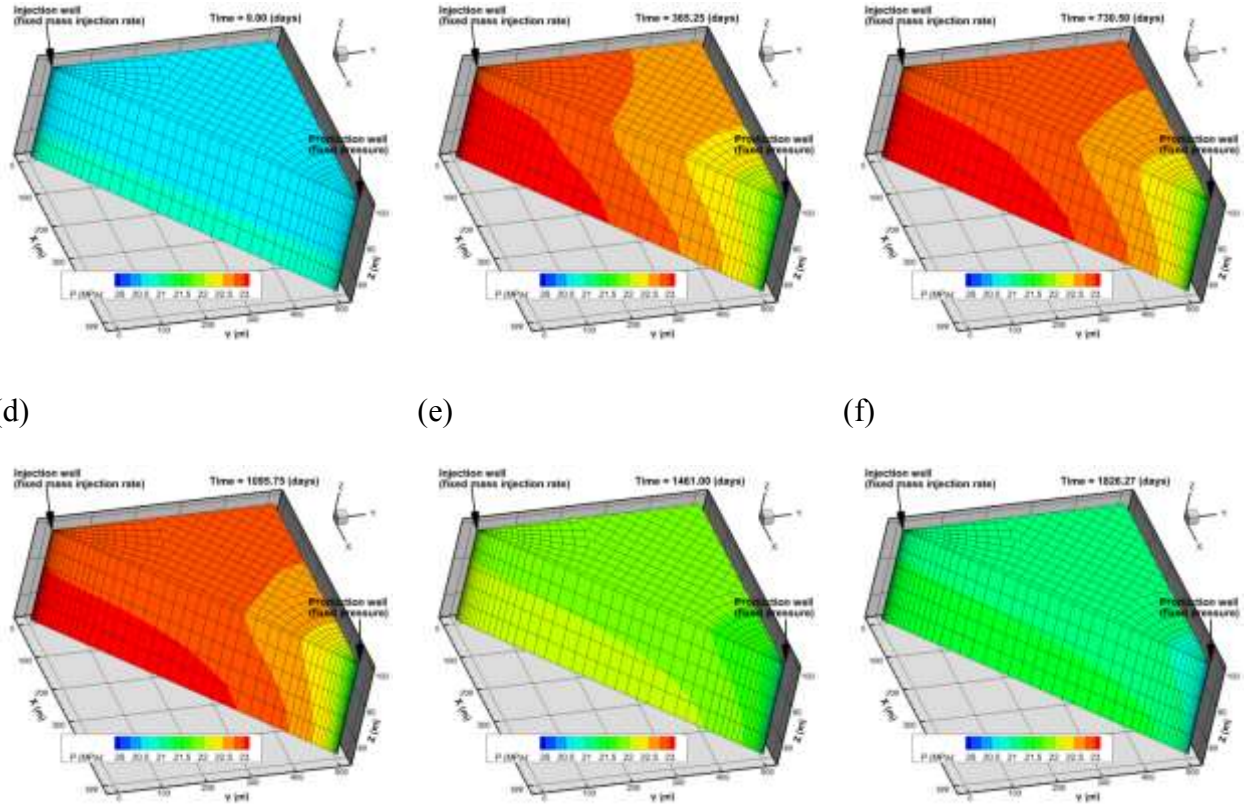

Figure 8.15. Simulated reservoir pressure distribution under miscible conditions at various time, (a) initial, (b) 1 year, (c) 2 years, (d) 3 years, (e) 4 years, and (d) 5 years.

(a) (b) (c)

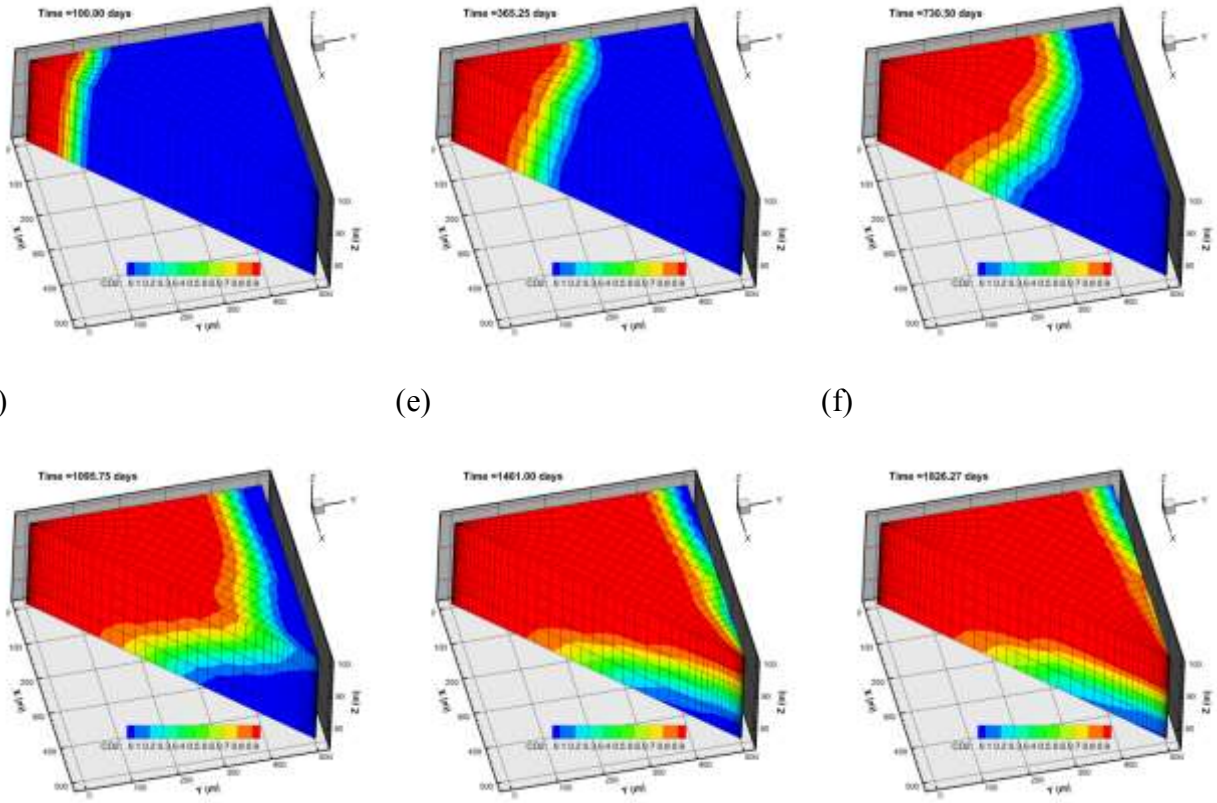

(d) (e) (f)

Figure 8.16. Calculated CO_2 mole fractions in the HC components (primary variables) under miscible conditions, (a) 100 days, (b) 1year, (c) 2 years, (d) 3 years, (e) 4 years, and (f) 5 years.

(a) (b) (c)

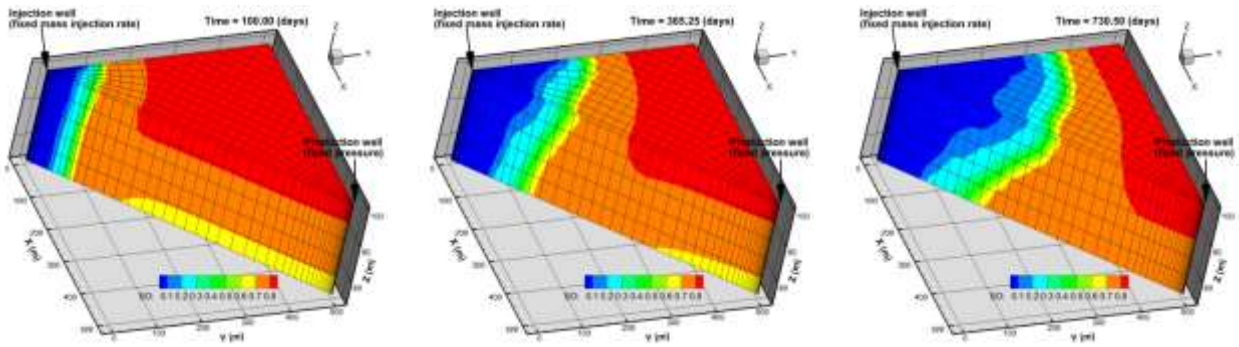

(d) (e) (f)

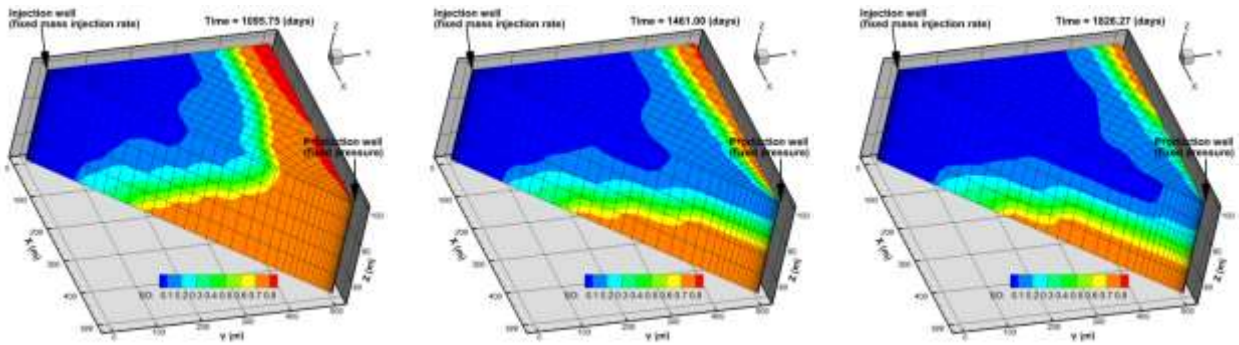

Figure 8.17. Calculated oil saturation in reservoir under miscible conditions at various times, (a) 100 days, (b) 1year, (c) 2 years, (d) 3 years, (e) 4 years, and (d) 5 years.

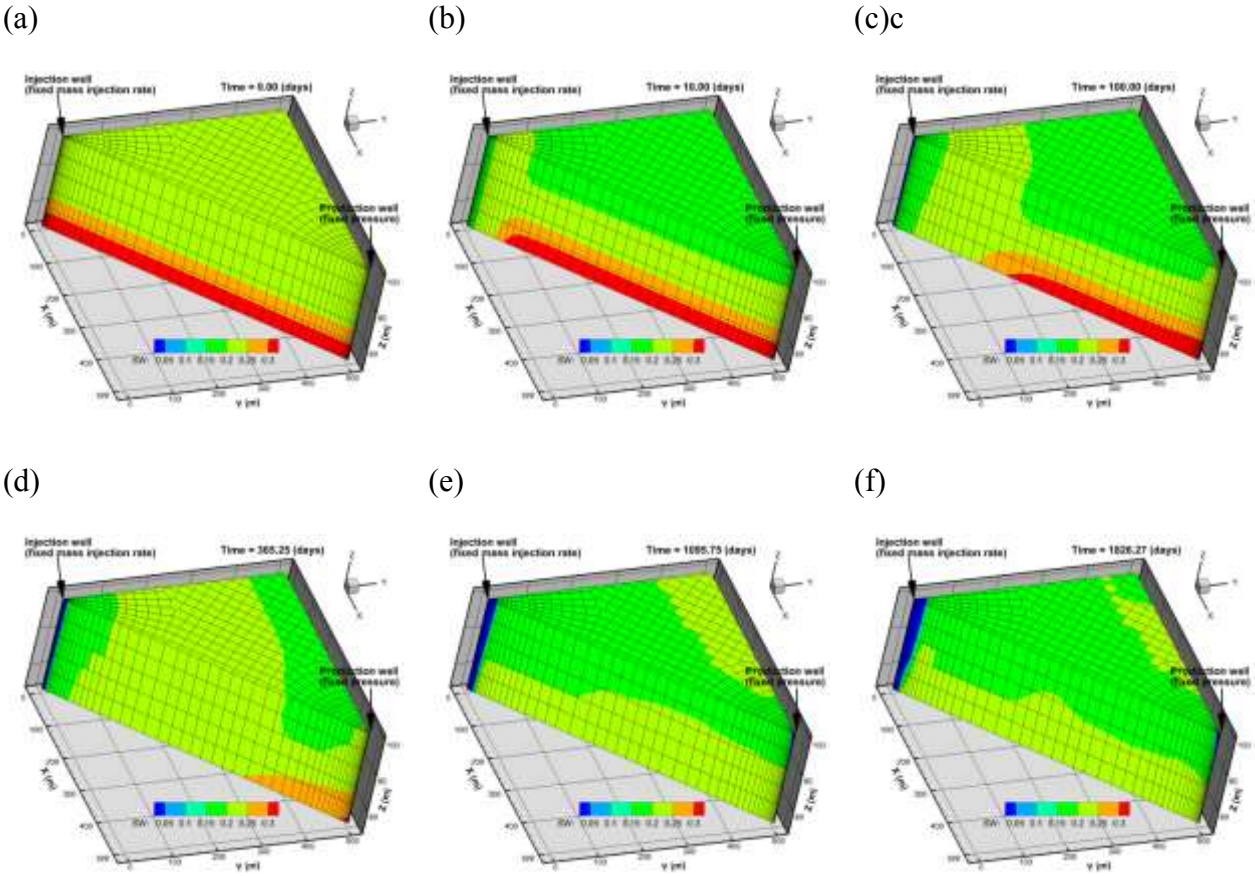

Figure 8.18. Calculated water phase saturation in reservoir under immiscible conditions at various times, (a)initial, (b) 10 days, (c) 100 days, (d) 1 years, (e) 3 years, and (f) 5 years.

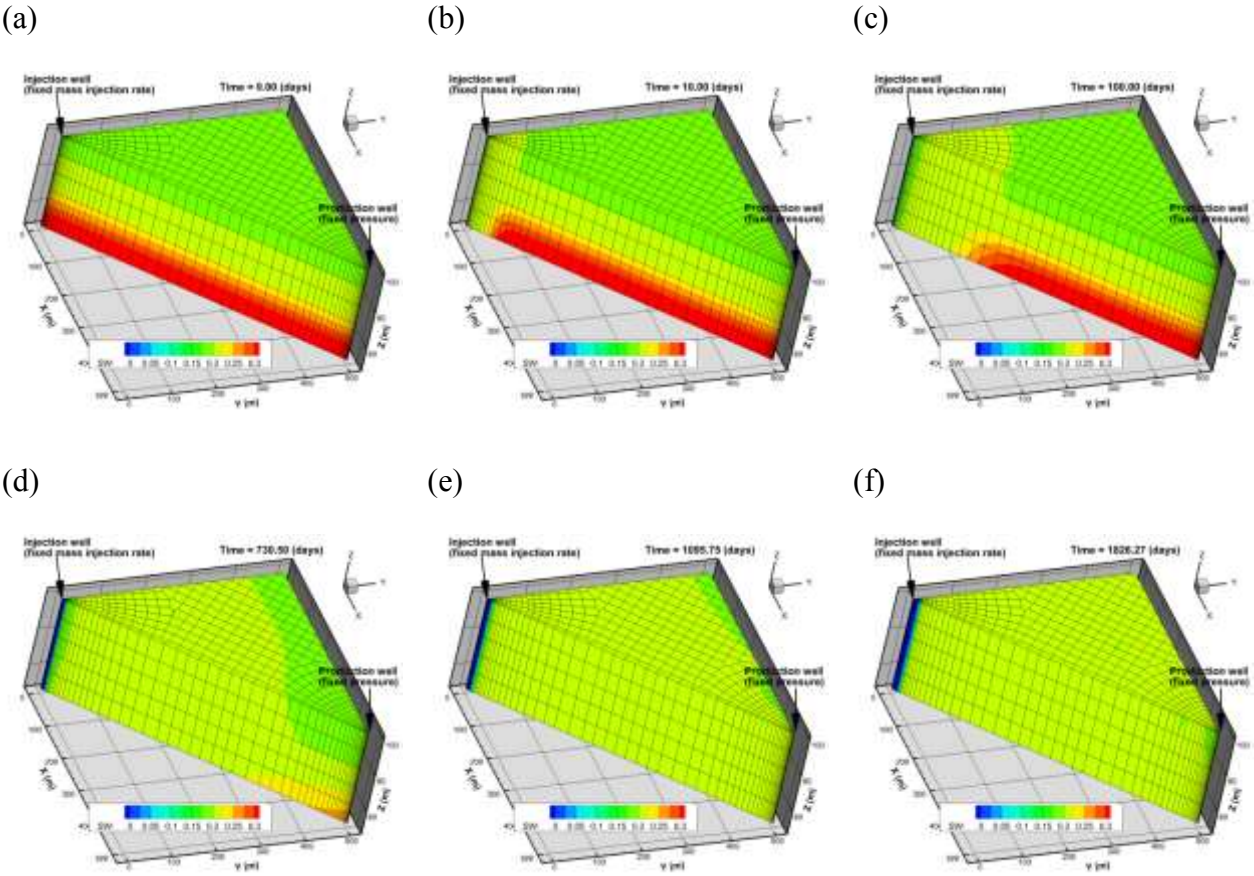

Figure 8.19. Calculated water phase saturation in reservoir under miscible conditions at various times, (a)initial, (b) 10 days, (c) 100 days, (d) 1 years, (e) 3 years, and (f) 5 years.

9. Conclusions

A new numerical reservoir simulator, TOGA (TOUGH Oil-Gas-Aqueous), has been developed. TOGA can be used for modeling non-isothermal flow and transport of water, CO_2, oil, and related gas components for applications including CO_2-enhanced oil recovery (CO_2-EOR) and geologic carbon sequestration in depleted oil and gas reservoirs.

TOGA has an internal database that stores the parameters of 20 components including H_2O, CO_2, common hydrocarbon components, and other gas components. Except for H_2O (default

component in any simulation), the user, in a simulation, can combine any number of the components from the list (or entered as hypothetical components with required parameters provided).

Each phase (O, G, or A) can appear or disappear according to the local pressure, temperature, and material composition in the given grid cell. Each component is allowed to exist in any stable phases (e.g., water can dissolve in gas or oil phase; HC components can dissolve in aqueous phase).

The model has been verified with other numerical codes and validated against the experiment data.

A hypothetical 3D CO_2 EOR problem has been simulated to demonstrate its capability for simulating three-phase, multiple component flow and transport often involved in CO_2-enhanced oil recovery (CO_2-EOR) and geologic carbon sequestration in depleted oil and gas reservoirs.

10. Acknowledgments

This work was funded by the Assistant Secretary for Fossil Energy, Office of Coal and

Power Systems through the National Energy Technology Laboratory, and by royalty funds administered by the Energy Geosciences Division of LBNL, and by Lawrence Berkeley National Laboratory under Department of Energy Contract No. DE-AC03-76SF00098. We thank Stefan Finsterle and Christine Doughty (LBNL) for internal reviews.

11. Nomenclature

d	molecular diffusivity	$m^2\ s^{-1}$
H	enthalpy	$J\ kg^{-1}$
Kh	Henry's coefficient	Pa
MW	molecular weight	$kg\ mole^{-1}$
NCG	non-condensible gas	
NEQ	number of equations per grid block	
NK	number of mass components (species)	
NKIN	number of mass components (species) in INCON file or block	
NPH	maximum number of phases present	
P	pressure	Pa
R	gas constant (8.31433 $J\ kg^{-1}\ ^{\circ}C^{-1}$)	$J\ kg^{-1}\ K^{-1}$
S	phase saturation	-
t	time	sec.
T	temperature	$^{\circ}C$, K
V	volume	m^3
$\overline{V_i}$	partial molar volume	$m^3\ mol^{-1}$
x	mole fraction in the liquid phase	-
X	mass fraction	-
y	mole fraction in the gas phase	-
Y	Y-coordinate	m

Z	Z-coordinate	m
Z	Z factor (compressibility factor)	-

Greek symbols

μ	dynamic viscosity	kg m^{-1} s^{-1}
ϕ	porosity	–
ρ	density	kg m^{-3}
τ	tortuosity	–

Subscripts and superscripts

aq	aqueous phase
g	gas phase
ig	ideal gas
l, liq	liquid
0	reference value
β	phase
κ	mass components

12. References

Battistelli, A. and Marcolini, M., 2009. TMGAS: a new TOUGH2 EOS module for the numerical simulation of gas mixtures injection in geological structures. International Journal of Greenhouse Gas Control, 3(4), pp.481-493.

Bottini, S.B. and Saville, G., 1985. Excess enthalpies for (water+ nitrogen)(g) and (water+ carbon dioxide)(g) at 520 to 620 K and up to 4.5 MPa. *The Journal of Chemical Thermodynamics*, *17*(1), pp.83-97.

Chung, T.-H., M. Ajlan, L.L. Lee, and K.E. Starling (1988). Generalized multiparameter correlation for nonpolar and polar fluid transport properties, *Ind. Eng. Chem. Res.*, *27*, 671–679.

Coats, K.H., 1980. An equation of state compositional model. Society of Petroleum Engineers Journal, 20(05), pp.363-376.

Cramer, S.D. (1982). The solubility of methane, carbon dioxide and oxygen in brines from 0 to 300 ˚C, *U.S. Bureau of Mines Report No. 8706*.

D'Amore, F., and A.H. Truesdell (1988). A review of solubilities and equilibrium constants for gaseous species of geothermal interest, *Sci. Geol. Bull.*, *41*(3–4), 309–332, Strasbourg, France.

Firoozabadi, A., D. L. Katz, H. Soroosh, and V. A. Sajjadian (1988). Surface tension of reservoir crude-oil/gas systems recognizing the asphalt in the heavy fraction. SPE Reservoir Engineering, February, 1988, pp.265-272.

Fenghour, A., Wakeham, W.A. and Watson, J.T.R., 1996a. Densities of (water+ methane) in the temperature range 430 K to 699 K and at pressures up to 30 MPa. *The Journal of Chemical Thermodynamics*, *28*(4), pp.447-458.

Fenghour, A., Wakeham, W.A. and Watson, J.T.R., 1996b. Densities of (water+ carbon dioxide) in the temperature range 415 K to 700 K and pressures up to 35 MPa. *The Journal of Chemical Thermodynamics*, *28*(4), pp.433-446.

Ghafoori, A., Shahbazi, K., Darabi, A., Soleymanzadeh, A. and Abedini, A., 2012. The experimental investigation of nitrogen and carbon dioxide water-alternating-gas injection in a carbonate reservoir. *Petroleum Science and Technology*, *30*(11), pp.1071-1081.

Jamili, A., 2010. Modeling effects of diffusion and gravity drainage on oil recovery in naturally fractured reservoirs under gas injection. Ph.D. Dissertation, University of Kansas, Lawrence, KS, 2010

Karacaer, C., 2007. Mixing issues in CO_2 flooding: comparison of compositional and extended black-oil simulators (Doctoral dissertation, Colorado School of Mines. Arthur Lakes Library).

Li, A., J. Lv, Y. Liu, S. Fu, Y. Lu, Y. Zhang, and X. Ren, 2016. Experimental investigation of CO_2-EOR in a compositional core with super-low permeable rocks. China Petroleum University-Qingdao.

McCain, William D. 1990. *The properties of petroleum fluids*. PennWell Books.

Nagarajan, N., Khaled A. M. Gasem, Robert L. Robinson Jr., Equilibrium phase compositions, phase densities, and interfacial tensions for carbon dioxide + hydrocarbon systems. 6. Carbon dioxide + n-butane + n-decane, J. Chem. Eng. Data, 1990, 35 (3), pp 228–231.

Nghiem, L.X., and Y.K. Li (1989), Phase-equilibrium calculations for reservoir engineering and compositional simulation. In Second International Forum on Reservoir Simulation, Alpbach, Austria, September 4-8.

NIST Standard Reference Database 69 –NIST Chemistry Web Book, http://webbook.nist.gov, (retrieved during May 2013).

Patel, M.R., Holste, J.C., Hall, K.R. and Eubank, P.T., 1987. Thermophysical properties of gaseous carbon dioxide-water mixtures. *Fluid phase equilibria*, *36*, pp.279-299.

Patel, M.R. and Eubank, P.T., 1988. Experimental densities and derived thermodynamic properties for carbon dioxide-water mixtures. *Journal of Chemical and Engineering Data*, *33*(2), pp.185-193.

Péneloux, A., Rauzy, E. and Fréze, R., 1982. A consistent correction for Redlich-Kwong-Soave volumes. *Fluid Phase Equilibria*, *8*(1), pp.7-23.

Peng, D.Y. and Robinson, D.B., 1976. A new two-constant equation of state. Industrial & Engineering Chemistry Fundamentals, 15(1), pp.59-64.

Poling, B.E., J.M. Prausnitz, and J.P. O'Connell (2000). *The properties of gases and liquids, fifth edition*, McGraw Hill, New York.

Press, W. H., S. A. Teukolsky, W. T. Vetterling, and B. P. Flannery, 1992. Numerical Recipes in FORTRAN The art of scientific computing (2nd edition). Cambridge University Press, ISBN 0-521-43064-X.

Pruess, K., C.M. Oldenburg and G.J. Moridis (1999). TOUGH2 User's Guide Version 2. E. O. Lawrence Berkeley National Laboratory Report *LBNL-43134*, 1999; and *LBNL-43134 revised).*

Pruess, K. and Spycher, N., 2007. ECO2N–A fluid property module for the TOUGH2 code for studies of CO 2 storage in saline aquifers. *Energy Conversion and Management*, *48*(6), pp.1761-1767.

Quiñones-Cisneros, S.E., Zéberg-Mikkelsen, C.K. and Stenby, E.H., 2000. The friction theory (f-theory) for viscosity modeling. Fluid Phase Equilibria, 169(2), pp.249-276.

Rachford Jr., H.H. and Rice, J.D. 1952. Procedure for Use of Electronic Digital Computers in Calculating Flash Vaporization Hydrocarbon Equilibrium. J Pet Technol 4 (10): 19, 3. SPE-952327.

Reagan, M.T. (2005). WebGasEOS 1.0 User Guide, Lawrence Berkeley National Laboratory Report *LBNL/PUB-3188*.

Sage, B.H. and Lacey, W.N., 1950. *Thermodynamic properties of the lighter paraffin hydrocarbons and nitrogen: monograph on API Research Project 37*. American Petroleum Institute.

Steffen, M. (1990). A simple method for monotonic interpolation in one dimension. Astronomy and Astrophysics. 239, pp. 443-450.

U.S. Department of Energy, Carbon Dioxide Enhanced Oil Recovery Untapped Domestic Energy Supply and Long Term Carbon Storage Solution, National Energy Technology Laboratory Report, 30 pp, 2010.

White, M.D. and Oostrom, O.M., 2000. Subsurface transport over multiple phases; Version 2.0; Theory Guide. Pacific Northwest National Laboratory.

White, M.D., Bacon, D.H., McGrail, B.P., Watson, D.J., White, S.K. and Zhang, Z.F., 2012. STOMP Subsurface Transport Over Multiple Phases: STOMP-CO2 and STOMP-CO2e Guide: Version 1.0 (No. PNNL-21268). Pacific Northwest National Laboratory (PNNL), Richland, WA (US).

Whitson, C.H. and Brule, M.R., 2000. Gas and Oil Properties and Correlations. *Phase Behavior*, *20*, pp.18-46.

Wormald, C.J., Lancaster, N.M. and Sellars, A.J., 1986. The excess molar enthalpies of {xH 2 O+(1− x) CO}(g) and {xH 2 O+(1− x) CO 2}(g) at high temperatures and pressures. *The Journal of Chemical Thermodynamics*, *18*(2), pp.135-147.

Yaws C.L., Miller, J.W., Shah, P.N., Schorr, G.R., and Patel, P.M. (1976), Correlation constants for chemical compounds, Chem. Eng. Sci., Vol. 83, No. 24, pp. 153 - 162.

Zakirov, I.V., 1984. PVT Relations in the System H_2O-CO_2 Under 300^oC and 400^oC at Pressure up to 1000 BAR. *Geokhimiya*, (6), pp. 805-811.

Zawisza, A., Malesińska B. Solubility of Carbon Dioxide in Liquid Water and of Water in Gaseous Carbon Dioxide in the Range 0.2–5 MPa and Temperatures up to 473 K. J. Chem. Eng. Data, 26 (1981), pp. 388–391.

Appendix A: Notes on INPUT format

TOGA uses the same input format as the standard TOUGH2 code (Pruess et al., 1999). However, there are many modifications (new input under standard TOUGH keywords) or new inputs (new keywords)which are described below:

A.1 Number of HC components under keyword: MULTI

Format (6I5)

NK, NEQ, NPH,NB,NKIN,NHCIN

The last parameter 'NHCIN' is a new input parameter indicates the number of HC components in INCON data, which allows the user to use the INCON data generated with less HC components (e.g., injection of one or more new components into the reservoir).

A.2 Tabular data of relative permeability and capillary pressure under keyword: ROCKS

Tabular data input of relative permeability and capillary function is offered in TOGA. This option is invoked by assigning IRP=14 (STONE I), 15 (STONE II), or 16 (BAKER). The data are organized as two groups, the water-oil group followed by the gas-oil group. The water-oil group has four columns of data:

S_w --water saturation (monotonically increasing);

$k_{rw}(S_w)$ --water relative permeability;

$k_{row}(S_w, S_g = 0)$ --oil relative permeability when only oil and water are present;

$P_{cwo}(S_w)$ --water capillary pressure vs. oil (Pa, nondecreasing).

The gas-oil group also has four columns of data:

S_g --gas saturation (monotonically increasing);

$k_{rg}(S_g)$ --gas relative permeability;

$k_{rog}(S_g, S_w = S_{wc})$ --oil relative permeability at connated water saturation;

$P_{cog}(S_g)$ --oil capillary pressure vs. gas (Pa, nondecreasing).

The first S_w data is the connated water saturation S_{wc}. The last value in column3 must be zero for both group. The first entry in column 3 of the water-oil group, $k_{row}(S_w = S_{wc}, S_g = 0)$, must equal to the first entry in column 3 of the oil-gas group, $k_{rog}(S_g = 0, S_w = S_{wc})$. Figure A-1 shows an example of such input.

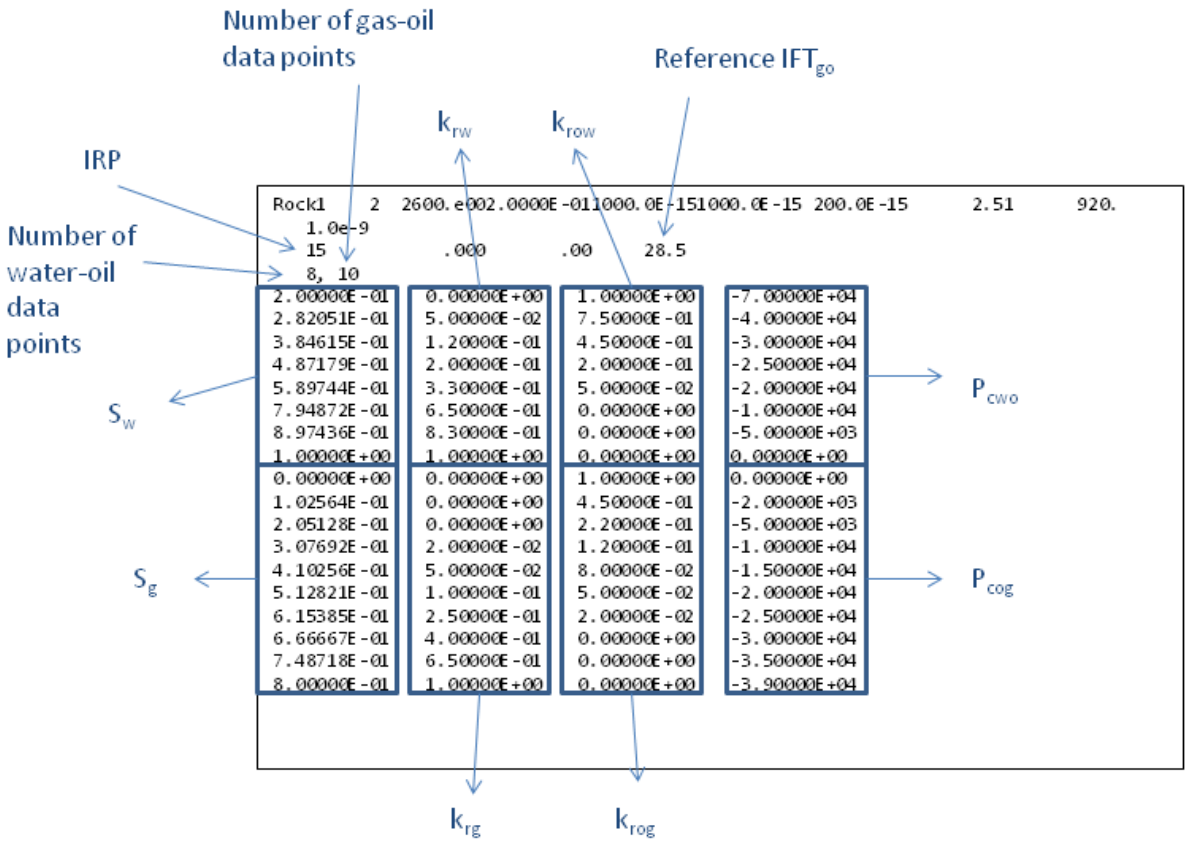

Figure A-1 Input of tabular relative permeability and capillary pressure data.

A.3 Define HC component types under keyword: CHEMP and the parameters of hypothetical components

The HC components involved in the model can be defined using the keyword 'CHEMP' in the input file. As shown in Figure A-2, the first line below CHEMP contains the number of HC components and the number of hypothetical components, separated by a comer. For those components that are included in the internal data bank (Table3.1), the user can simply list their symbols in the input file to define them. The hypothetical component refers to those components that are not included in the internal data bank (e.g., a lumped component), for which the unique symbol must be started with '+' and the corresponding molecular weight (g/mol) must be provided in the same line (columns 9-19). Three rows of additional parameters for that

component must also be provided right below that component. The first row of which is the critical parameters for that component (Figure A-2). The second row is the three parameters used to calculate the viscosity of the component using equation (3-15). The third row is the empirical parameters used to calculate the specific enthalpy of the component as a function of temperature under low pressure (ideal gas). If there are multiple hypothetical components, just repeat the input in the similar manner. The last two entries of 'CHEMP' section is the molecular weight (g/mol) and the specific density of C7+ components which is need in the calculation of equilibrium coefficient using empirical K-value method.

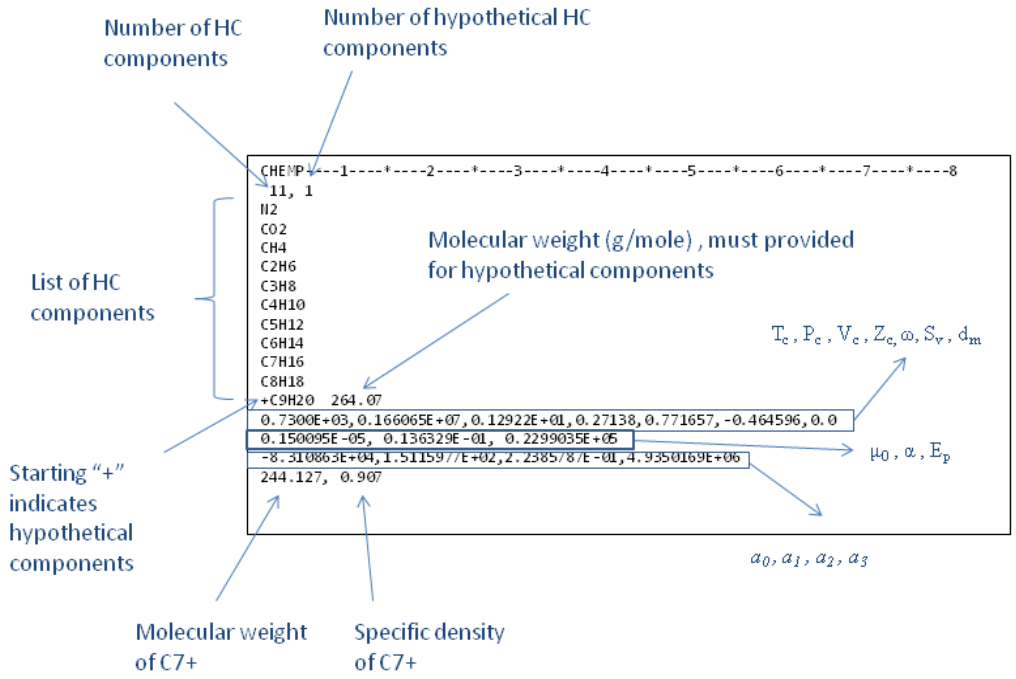

Figure A-2. CHEMP input: An example of 11 HC components with one hypothetical component

A.4. Define one-way connection under keyword: CONNE

ISO is the index used in TOUGH to determine which direction the connection is so that the proper directional permeability will be used for the connection, e.g., k_x (ISO=1), k_y (ISO=2), and

k_z (ISO=3). TOGA allows the user to define one-way connections by assigning ISO with 4 or 5 (Figure A-3). As shown in Figure A-3, if ISO is 4, the flow is only allowed from Cell 2 to Cell 1 whereas the flow is allowed only from Cell 1 to Cell 2 if ISO is 5. Internally, ISO-3 will be used in selection of the permeability in the case that ISO is larger than 3. In addition, if the connection is included in the list of COFT, ISO>3 will also make the cumulative oil and gas flow output to be corresponding to the volumes of oil and gas at the standard conditions (see the description of COFT output for details).

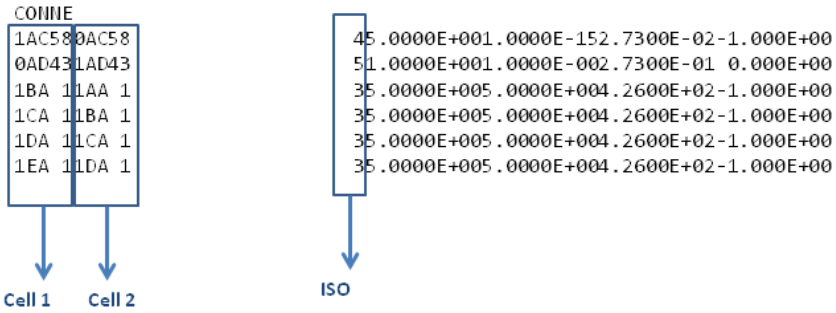

Figure A-3. CONNE input: An example of two one-way connections. "ISO=4" indicates that flow is allowed only from Cell 2 ("0AC58") to Cell 1 ("1AC58") whereas "ISO=5" indicates that flow is allowed only from Cell 1 ("0AD43") to Cell 2 ("1AD43"). Note that ISO-3 will be used to select which permeability defined in ROCKS.

A.5. Parameters under keyword: SELEC

IE(2) = 0 (default, PR)
1 (PR)
2 (RK, not tested in this development)
3 (SRK, not tested in this development)

IE(8) = 0 (gas-oil K-values are determined using Eq.4-8, no iteration in flash calculation)
>0 (gas-oil K-values are iteratively calculated until the fugacities are equal between gas and oil phases; IE(8) is the number of maximum iterations)

IE(11) = 0 (default, volume shift technique is used in calculation of gas (or oil) density
1 (volume shift technique will be disabled)

A.6. Define standard pressure and temperature under keyword: PROPT

The standard pressure and temperature used to calculate the cumulative gas and oil volume production/injection can be entered by using the keyword PROPT (Figure A-5) if the user want evaluate the gas and oil volume at different conditions from the default conditions (P = 101325 Pa and T = 15^{o}C).

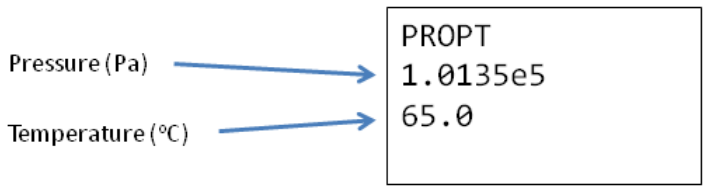

Figure A-5 Input for assigning standard pressure and temperature at which the cumulative oil and gas volume (production) will be evaluated.

A.7. New parameters under keyword: INCON

A new three character keyword immediately followed the keyword "INCON" is used to describe the type of INCON. If it is "EOR" (the default), the primary variables are as listed in Table 4.1. The other types of INCON are described below:

NAQ: As shown in Table A-1, the major difference is the second primary variable, which is the mole fraction of water in the mixture (G, O, or G+O), the total mole fraction of HC components in aqueous phase (W), or the aqueous phase saturation (W+G, W+G, or W+G+O), respectively. In addition, the "J-component" is always the NHCth component (i.e., ID of "J-component" will

be ignored) in this type of INCON. The first primary variable is always the total pressure. Therefore, this type of INCON should not be used directly for nonisothermal simulations.

TMV: This is TMVOC style of INCON and shown in Table A-2. Different set of primary variables is used for each of seven phase conditions. Note that, in this case, the old phase ID system (PID) is used for the CID input in the INCON. Similar to the case of NAQ type, the ID of "J-component" is ignored and this INCON type should not be used directly for nonisothermal simulations.

CO2: This is ECO2N style of INCON. The input of salt will be ignored because the salt has not been included in the current TOGA. All other HC components are assumed to be zero initially in this case. Similar to the case of NAQ type, the ID of "J-component" is ignored and this INCON type should not be used directly for nonisothermal simulations.

*** (* can be any character except space, e.g., TAB): This is an option for a user to provide initial conditions through a separated file (e.g., TAB.incon). If TOGA find the type of INCON is not one of those described above, it will try to search the file "***.incon" (e.g., TAB.incon) in the working file folder. If found, TOGA will read CID and the primary variables (as described in Table 4.1) grid cell by grid cell from the file. The order of grid cells must been the same as those listed in ELEME section of input file. The ID of "J-component" must be the default value (NHC-1) in this case.

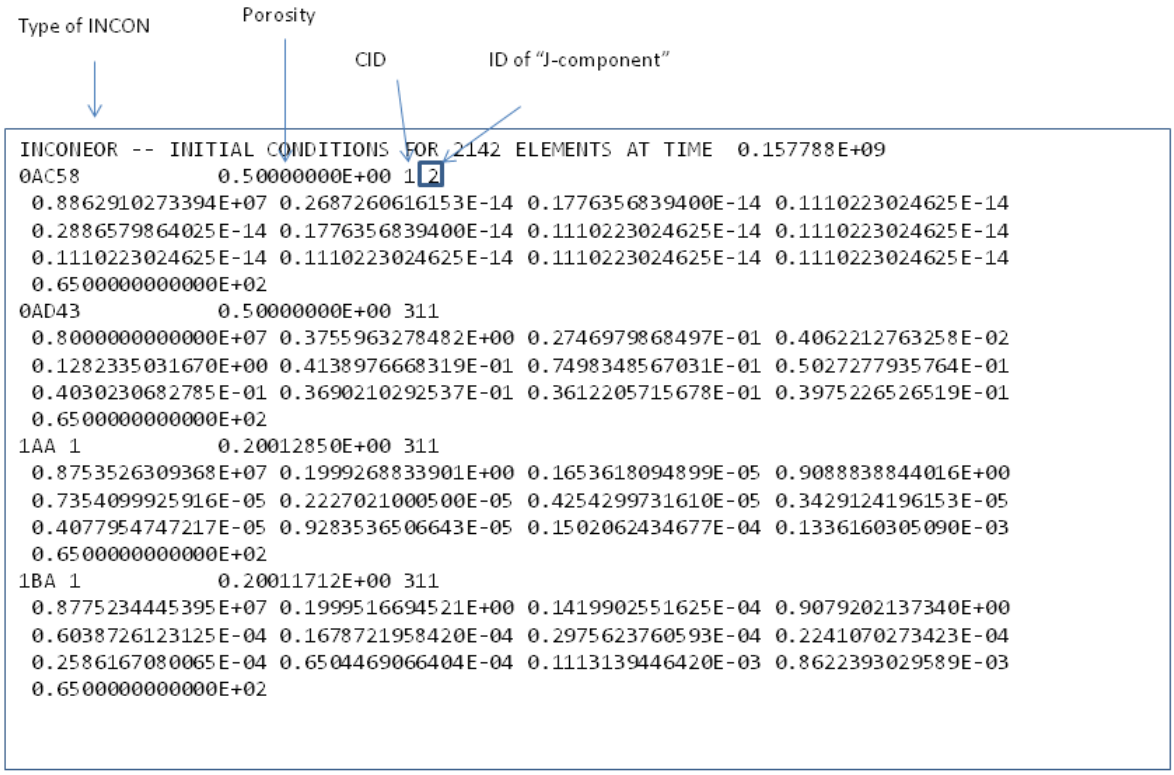

Figure A-6 Input for assigning type of INCON, C ID, and the ID of "J-component".

Table A-1 Primary variables in INCON with type of "NAQ"

Phase conditions				Primary variables			
Phase category	CID	PID	Actual Phase	1	2	3 to NHC+1	NHC+2
Non-aq only	1	1	Gas only (G)	P	X_N^W	$Z_i (i = 1,\ldots, NHC-1)$	T
		3	Oil only (O)				
		5	Gas and oil (G+O)				
Aqueous only	2	2	Water only (W)		X_w^{HC}		
Two or more phases	3	4	Water and gas (W+G)		S_w		
		6	Water and oil (W+O)				
		7	Three phase (W+G+O)				

Table A-2 Primary variables in INCON with type of "TMV"

Phase conditions			Primary variables				
Phase category	CID	Actual Phase	1	2	3 to NHC	NHC+1	NHC+2
Non-aq only	1	Gas only (G)	P	X_1^g	$X_i^g\left(i=2,\ldots,NHC-1\right)$	X_{NHC}^g	T
	3	Oil only (O)		X_1^o	$X_i^o\left(i=2,\ldots,NHC-1\right)$	X_{NHC}^o	
	5	Gas and oil (G+O)		X_1^g	$X_i^g\left(i=2,\ldots,NHC-1\right)$	S_o	
Aqueous only	2	Water only (W)		X_1^w	$X_i^w\left(i=2,\ldots,NHC-1\right)$	X_{NHC}^w	
Two or more phases	4	Water and gas (W+G)		X_1^g	$X_i^g\left(i=2,\ldots,NHC-1\right)$	S_w	
	6	Water and oil (W+O)		X_1^g	$X_i^g\left(i=2,\ldots,NHC-1\right)$	S_o	
	7	Three phase (W+G+O)		S_g	$X_i^g\left(i=2,\ldots,NHC-1\right)$	S_w	

A.8. User specified binary interaction coefficients under keyword: BIJSS

If a user want to use his/her own set of binary coefficients for the state of equation instead of those in the internal databank, the user can do so by using the keyword BIJSS in the main input file (Figure A-6). The number of components under BIJSS must be equal to either NK-1 (excluding H_2O) or NK (including H_2O). The elements in the binary interaction coefficient matrix should be ordered consistently with the components defined under CHEMP and separated by a comer. The example shown in Figure A-6 has 3 HC components (CO2, C4, and C10). As a result, the binary interaction coefficients of the HC components with H_2O will be taking from the internal databank in this case.

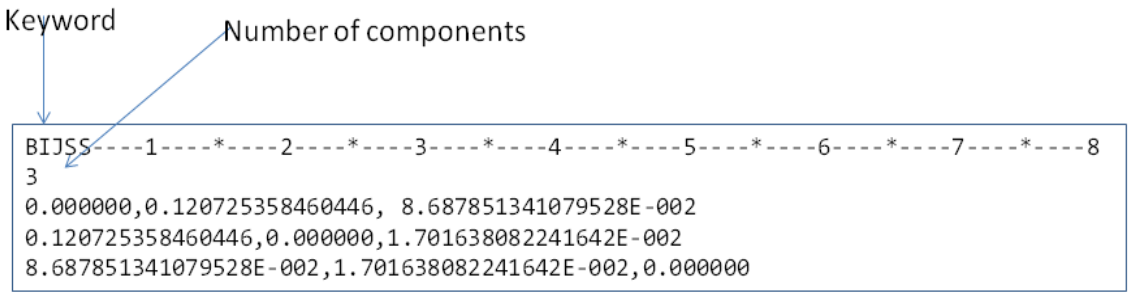

Figure A-6 An example of entering binary interaction coefficients using keyword BIJSS

A.9. User specified critical parameters under keyword: PCTCW

If a user want to use his/her own set of critical parameters for the involved components instead of those in the internal databank, the user can do so by using the keyword PCTCW in the main input file (Figure A-7). The number of components under PCTCW must be equal to either NK-1 (excluding H_2O) or NK (including H_2O). Each row consists of critical pressure, critical temperature, eccentric coefficient, and molecular weight, separated by a comer. The rows of data should be ordered consistently with the components defined under CHEMP. The example shown in Figure A-7 has 3 HC components (C1, C4, and C10). As a result, the critical parameters of H_2O will be taking from the internal databank in this case.

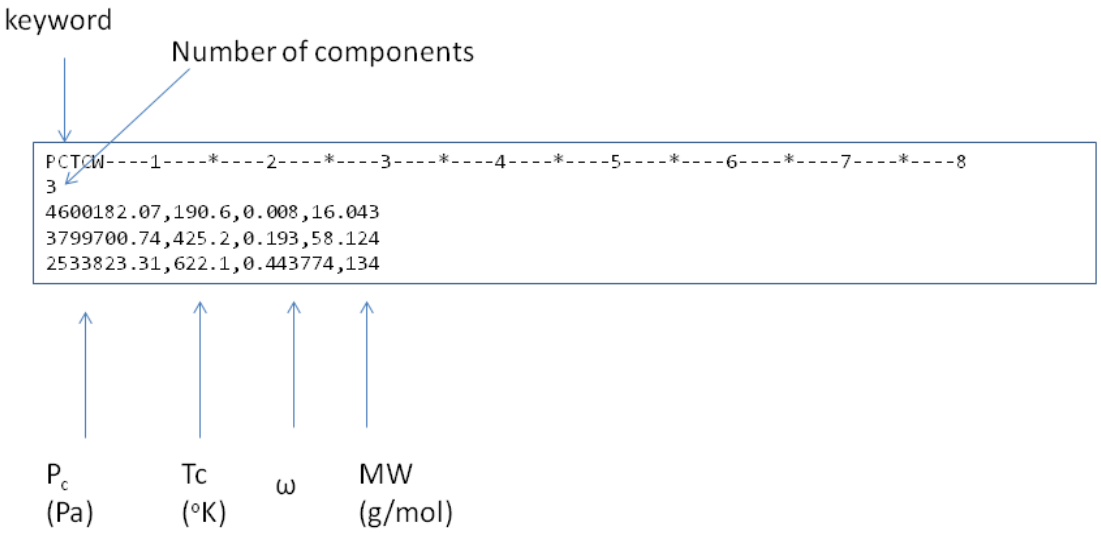

Figure A-7 An example of entering critical parameters using keyword PCTCW

Appendix B: Notes on OUTPUT format

The followings are brief descriptions of some new or modified output formats that are different from or not existed in the standard TOUGH2 output files (Pruess et al., 1999).

B.1. COFT: flow rate output of selected connections

COFT is an output file (fixed filename) of TOUGH2 for the users to check time series of the flow rates through the user specified connections. TOGA uses the same structure of COFT file as standard TOUGH2. The first column of data is the count of records and the second is the simulation time in seconds. The rest is repeated for each connection starting with ID of the connection. The variables outputted by TOGA for each connection in COFT file are described in Table B-1.

Table B-1 Variables for one connection in COFT file used by TOGA

Variable	Unit	Note
ID of the connection	-	The component flow rates are calculated as summation of the flow rates per component in all phases. If ISO of the connection is larger than 3, a flash calculation at standard P and T will performed for the mixture of all components excluding H_2O to get corresponding gas volume and oil volume at that conditions. Therefore, the volumetric flow rates and cumulative volumes are evaluated at the given standard conditions, not at local conditions in the simulation.
Gas phase flow rate	kg/s	
Aqueous phase flow rate	kg/s	
Oil phase flow rate	kg/s	
Energy flow rate	W	
H_2O (component) flow rate	kg/s	
Gas component flow rate	kg/s or m^3/s if ISO>3	
C4+ component flow rate	kg/s or m^3/s if ISO>3	
Cumulative H_2O	kg	
Cumulative gas	kg or m^3 if ISO>3	
Cumulative oil	kg or m^3 if ISO>3	

B.2. FOFT: state variables at the selected grid cells

FOFT is an output file (fixed filename) of TOUGH2 for the users to check time series of the state variables at the user specified grid cells. TOGA uses the same structure of FOFT file as standard TOUGH2. The first column of data is the count of records and the second is the simulation time in seconds. The rest is repeated for each grid cell starting with ID of the cell. The variables outputted by TOGA for each cell in FOFT file are described in Table B-2.

Table B-2 Variables for one grid cell in FOFT file used by TOGA

Variable	Unit
ID of the grid cell	-
CID	-
Pressure	Pa
Temperature	^oC
Gas phase saturation	m^3/m^3
Oil phase saturation	m^3/m^3
Mole fraction of HC components in aqueous phase	mole/mole
Mole fraction of H_2O vapor in gas phase	mole/mole
Gas phase density	kg/m^3

Aqueous phase density	kg/m^3
Oil phase density	kg/m^3

B.3. mole fractions in various phases

Like any standard TOUGH2 code, TOGA produces standard output at user-specified simulation times or time steps. This output includes a complete cell-by-cell report of thermodynamic state variables (B-1). In addition to this, TOGA also provides a complete cell-by-cell report of mole fractions in different phases, namely, gas, oil, aqueous, or non-aqueous phase. Each phase could be either real or hypothetical (not stable under local conditions). Figures B-2, B-3, B-4, and B-4 show an example of such output.

```
OUTPUT DATA AFTER (  70,  3)-2-TIME STEPS                                              THE TIME IS  0.16000E+02 DAYS
 @@@@@@@@@@@@@@@@@@@@@@@@@@@@@@@@@@@@@@@@@@@@@@@@@@@@@@@@@@@@@@@@@@@@@@@@@@@@@@@@@@@@@@@@@@@@@@@@@@@@@@@@@@@@@@@@@@@@@@@@

  TOTAL TIME     KCYC   ITER  ITERC   KON                                              MAX. RES.     NER    KER       DELTEX
  0.13824E+07     70      3    229     2                                               0.45762E-10     1      2       0.36123E+05

     DX1M        DX2M        DX3M        DX4M        DX5M        DX6M        DX7M        DX8M        DX9M       DX10M       DX11M
 0.33889E+05 0.43121E-05 0.14573E-04 0.31345E-05 0.00000E+00
 @@@@@@@@@@@@@@@@@@@@@@@@@@@@@@@@@@@@@@@@@@@@@@@@@@@@@@@@@@@@@@@@@@@@@@@@@@@@@@@@@@@@@@@@@@@@@@@@@@@@@@@@@@@@@@@@@@@@@@@@


 ELEM.  INDEX      P           T          SG          SW         SO          PCWG        PCOG       XVOCW        DGAS        DNAPL        Daq
                  (PA)      (DEG-C)                                          (PA)        (PA)    (MASS FRACT.)  (KG/M**3)   (KG/M**3)   (KG/M**3)

 a 111     1 0.21605E+08 0.71111E+02 0.40726E-02 0.20103E+00 0.79490E+00 0.00000E+00 0.00000E+00 0.18520E-02 0.17796E+03 0.63988E+03 0.98643E+03
 a 211     2 0.21588E+08 0.71111E+02 0.46748E-02 0.20103E+00 0.79430E+00 0.00000E+00 0.00000E+00 0.18511E-02 0.17779E+03 0.63999E+03 0.98642E+03
 a 311     3 0.21553E+08 0.71111E+02 0.58957E-02 0.20103E+00 0.79307E+00 0.00000E+00 0.00000E+00 0.18494E-02 0.17745E+03 0.64021E+03 0.98641E+03
 a 411     4 0.21500E+08 0.71111E+02 0.77407E-02 0.20104E+00 0.79122E+00 0.00000E+00 0.00000E+00 0.18468E-02 0.17692E+03 0.64056E+03 0.98639E+03
 a 511     5 0.21427E+08 0.71111E+02 0.10219E-01 0.20105E+00 0.78873E+00 0.00000E+00 0.00000E+00 0.18432E-02 0.17620E+03 0.64103E+03 0.98636E+03
 @@@@@@@@@@@@@@@@@@@@@@@@@@@@@@@@@@@@@@@@@@@@@@@@@@@@@@@@@@@@@@@@@@@@@@@@@@@@@@@@@@@@@@@@@@@@@@@@@@@@@@@@@@@@@@@@@@@@@@@@
```

Figure B-1 an example of standard output of cell-by-cell thermodynamic state variables

```
>>>>>>>>>> Mole FRACTIONS IN THE  OIL  PHASE <<<<<<<<<<

ELEM. INDEX  oXWAT      o2_CH4      o3_C4H10    o4_C10H22   o5_SUMMOLEF Z
a 111   7  0.13466E-04 0.52818E+00 0.10580E+00 0.36600E+00 0.42117E-09 0.80622E+00
a 211   7  0.13476E-04 0.52789E+00 0.10584E+00 0.36625E+00 0.46566E-09 0.80584E+00
a 311   7  0.13498E-04 0.52728E+00 0.10594E+00 0.36677E+00 0.56281E-09 0.80506E+00
a 411   7  0.13532E-04 0.52635E+00 0.10609E+00 0.36755E+00 0.72746E-09 0.80387E+00
a 511   7  0.13578E-04 0.52508E+00 0.10629E+00 0.36862E+00 0.98268E-09 0.80224E+00
```

Phase ID (PID)

Figure B-2 an example of standard output of cell-by-cell mole fractions in oil phase and the compressibility coefficient of oil. PID=7 indicates that all three phases (G, O, and A) are real under local conditions.

```
                              >>>>>>>>>> Mole FRACTIONS IN THE  GAS  PHASE <<<<<<<<<<

ELEM. INDEX  gXWAT      g2_CH4      g3_C4H10    g4_C10H22   g5_SUMMOLEF g6_Z-FACTOR
a 111   7  0.15131E-02 0.94658E+00 0.38939E-01 0.12969E-01 0.33562E-09 0.84816E+00
a 211   7  0.15143E-02 0.94661E+00 0.38929E-01 0.12944E-01 0.38163E-09 0.84812E+00
a 311   7  0.15167E-02 0.94668E+00 0.38910E-01 0.12894E-01 0.48183E-09 0.84805E+00
a 411   7  0.15205E-02 0.94678E+00 0.38880E-01 0.12817E-01 0.65096E-09 0.84793E+00
a 511   7  0.15257E-02 0.94692E+00 0.38840E-01 0.12713E-01 0.91196E-09 0.84778E+00
```

Phase ID (PID)

Figure B-3 an example of standard output of cell-by-cell mole fractions in gas phase and the compressibility coefficient of oil. PID=7 indicates that all three phases (G, O, and A) are real under local conditions.

```
                              >>>>>>>>>> Mole FACTIONS IN THE AQUEOUS PHASE <<<<<<<<<

ELEM. INDEX  aXWAT      a2_CH4      a3_C4H10    a4_C10H22   a5_SUMMOLEF
a 111   7  0.99794E+00 0.20524E-02 0.71918E-05 0.82062E-07 0.00000E+00
a 211   7  0.99794E+00 0.20515E-02 0.71945E-05 0.82065E-07 0.00000E+00
a 311   7  0.99794E+00 0.20495E-02 0.72002E-05 0.82070E-07 0.00000E+00
a 411   7  0.99795E+00 0.20465E-02 0.72089E-05 0.82077E-07 0.00000E+00
a 511   7  0.99795E+00 0.20425E-02 0.72207E-05 0.82088E-07 0.00000E+00
```

Phase ID (PID)

Figure B-4 an example of standard output of cell-by-cell mole fractions in aqueous phase and the compressibility coefficient of oil. PID=7 indicates that all three phases (G, O, and A) are real under local conditions.

```
                                >>>>>>>>>> Mole FRACTIONS IN THE  NAQ  PHASE <<<<<<<<<<

ELEM. INDEX    CH4          C4H10        C10H22
a 111    7  0.53016E+00 0.10549E+00 0.36435E+00
a 211    7  0.53016E+00 0.10549E+00 0.36436E+00
a 311    7  0.53014E+00 0.10549E+00 0.36437E+00
a 411    7  0.53011E+00 0.10549E+00 0.36440E+00
a 511    7  0.53005E+00 0.10550E+00 0.36445E+00
```

Phase ID (PID)

Figure B-5 an example of standard output of cell-by-cell mole fractions in non-aqueous phase and the compressibility coefficient of oil. PID=7 indicates that all three phases (G, O, and A) are real under local conditions. These mole fractions are calculated based on HC components only (i.e., excluding water).